Institute for Theoretical Physics

University of Cologne

Bachelorthesis

Persistence Statistics of Electricity Price Time Series

First Revisor: Prof. Dirk Witthaut
Second Reivsor: Prof. Johannes Berg

Eva Sophia Mix
E-Mail: eva.mix@smail.uni-koeln.de
Matriculation Number 7307221

Cologne, 7th August 2020

Eidesstattliche Erklärung

Hiermit versichere ich, Eva Sophia Mix, geboren am 25.08.1994, Matrikelnummer 730211, an Eides statt, dass ich die vorliegende Arbeit selbstständig und ohne die Benutzung anderer als der angegebenen Hilfsmittel angefertigt habe. Alle Stellen, die wörtlich oder sinngemäß aus veröffentlichten und nicht veröffentlichten Schriften entnommen wurden, sind als solche kenntlich gemacht. Die Arbeit ist in gleicher oder ähnlicher Form oder auszugsweise im Rahmen einer anderen Prüfung noch nicht vorgelegt worden. Ich versichere, dass die eingereichte elektronische Fassung der eingereichten Druckfassung vollständig entspricht.

Köln, den 7. August 2020

Eva Sophia Mix

Contents

List of Figures

1 Introduction

Renewable power supply is a key element for mitigating climate change and a logical starting point towards a sustainable way of life and economy. It can be used to electrify other energy consuming sectors apart from electricity itself [50]. In the last decades the share of renewable energy in the German power supply increased from 3.4% in 1990 to 37.8% in 2018 [6] and is planned to further increased [4, 5, 19]. Renewable energy influences the optimal grid construction [11, 12, 51], the grid stability [24, 66], the need for backup and storage technologies [19, 24] and wholesale electricity prices [10, 25]. To estimate the weight of these aspects the statistical properties of renewable power generation need to be well understood.

Wind and solar power generation are highly variable, as they dependent on weather conditions. Solar power generation mostly depends on season and daytime [65], wind power generation exhibits more irregular variations [50] with little seasonal impact and large periods of high and low wind power generation [62]. In particular, the likeliness of such long periods is significantly larger than predicted by an exponential distribution, which describes the waiting time distribution in simple stochastic processes. Especially long periods of low wind power generation are crucial for a reliable supply with electric energy. They cannot be covered by the current and planned storage infrastructures and thus require dispatchable backup power plants.

Therefore, the variable feed-in of renewable power, especially wind power, has an important impact on the electricity market prices. This leads to the question whether the electricity price time series displays similar patterns as the wind power generation time series. Does large persistence of high or low wind power generation manifest in large persistence of low or high electricity prices? Is the persistence statistic of electricity prices heavy tailed? I will study this question by analyzing normalized time series of the day-ahead wholesale electricity prices.

For a start, I will review some fundamental aspects of stochastic processes and data analysis in chapter 2 and discuss renewable energy systems in chapter 3. I will then analyze the wholesale electricity price time series for the German market in chapter 4. I will start the analysis by taking a closer look at possible factors influencing the pricing of electricity. Electricity prices display strong daily, weekly and seasonal patterns, which proofs to be problematic in the further analysis. To circumvent this problem, I will introduce and compare different normalization methods to remove trends and recurring patters. For normalized time series I will calculate the waiting time distribution of high and low price states and compare it to an exponential maximum-likelihood fit and the kurtosis of an exponential distribution.

2 Stochastic Basics

Today a world without stochastics is hard to imagine, but there has been a time where mathematicians believed it was inherent to random phenomena that they cannot be mathematized. The beginning of the scientific study of probabilities is considered to be the correspondence between Blair Pascal and Pierre Fermat in 1654. Starting from the approach to predict chances in gambling, today there is a broad axiomatic foundation for probability theory.

Stochastics can be divided into two parts. Probability theory, which studies random experiments on the basis of assumed to be known mathematical models and statistics, which analyses data with the help of stochastic models. Statistics is one of the, if not the most common application of modern mathematics. Stochastic descriptions are used for a whole variety of topics. In quantum mechanics probability is a constitutive element with no deterministic equivalent [47].

Particularly for this thesis basic stochastic concepts are of central importance. To analyze patterns in velocities of wind and electricity prices concepts of probability theory are needed. Therefore, this chapter lays the foundation for the following chapters, especially the data analysis in chapter 4.

2.1 Fundamental Terms

This section concentrates on the basic concepts of probability, providing the fundamentals for the analysis of stochastic processes and time series in this thesis.

2.1.1 Probability Space

A probability space is a mathematical concept for random experiments describing observable outcomes of an experiment. It is a measurable space and is given by $(\Omega, \mathcal{F}, P)$, where Ω is the sample space, $\mathcal{F}$ is the system of all possible outcomes and P is the probability distribution. To understand this definition I will introduce the parts it consists of.

2.1.1.1 Sample Space

The sample space $\Omega \neq \emptyset$ is interpreted as the set of all possible outcomes of a random phenomenon. The different possible outcomes are the elements of the sample space and are called elementary events. The elementary events themselves are represented by $\omega \in \Omega$ [16]. It is important to note that the sample space is restricted to the extract of reality which is important to the experiment, i.e. when rolling a dice it is only important which side it shows and not the exact place on the table it comes to rest at. This reduction allows to concentrate on the crucial parts of the experiment. Therefore it is important to decide which idealizing assumptions can be made when modeling Ω [23]. Furthermore, it is often not even relevant which exact elementary event occurs, but only a certain subset of all possible results is relevant. This is where $\mathcal{F}$ comes in.

2.1.1.2 System of all Possible Outcomes $\mathcal{F}$

When defining $\mathcal{F}$ the aim is to define it in a way that it is possible to map every observable outcome $A \in \mathcal{F}$ to a probability $P(A)$. If Ω is countable $\mathcal{F}$ can be chosen as equal to the power set $\mathcal{P}(\Omega)$, which is the set of all subsets of Ω. However, Ω often is not countable, therefore it is necessary to be a bit more careful when defining $\mathcal{F} \subset \mathcal{P}(\Omega)$ [23].

Be $\Omega \neq \emptyset$. A set $\mathcal{F} \subset \mathcal{P}(\Omega)$ needs to have the following properties:

(a) $\Omega \in \mathcal{F}$

(b) $A \in \mathcal{F} \Rightarrow A^C := \Omega \setminus A \in \mathcal{F}$ (logical negation)

(c) $A_1, A_2, ... \in \mathcal{F} \Rightarrow \cup A_i \in \mathcal{F}$ (logical or) [16].

A set $\mathcal{F}$ with these properties is called σ-algebra. The elements $A \in \mathcal{F}$ are called measurable sets or events.

The given requirements for $\mathcal{F}$ are always given for physical application, they are just briefly mentioned for mathematical completeness.

2.1.1.3 Probability Distribution P

A function $P : \mathcal{F} \rightarrow [0, 1]$ is called probability distribution or probability measure. It maps every outcome $A \in \mathcal{F}$ to its probability of occurrence $P(A)$. This function is crucial for the creation of a good model for random experiments, because the probability mass function P holds all the important information about the respective random event [23].

The fundamental properties of a probability measure are:

(i) $P(\Omega) = 1$

(ii) $P(A^C) = 1 - P(A)$

(iii) $A \subset B \Rightarrow P(A) \leq P(B)$

(iv) $P(A_1 \cup \ldots A_n) \leq \sum_{i=1}^{n} P(A_i)$

For this properties independence, respectively dependence, between outcomes is important and will be discussed in section 2.1.5.1. More details about P can, for example, be found in the books [23] and [16]. Probability distributions can be distinguished between the continuous and the discrete case. The different types of probability distributions will be discussed in section 2.1.3.

2.1.2 Random Variables

Random variables are a useful tool for describing random events. Random variables can either represent possible outcomes of a future random experiment, or they also can represent possible outcomes of an experiment which has already been done. Therefore, they can describe a random process or can represent incomplete knowledge of a quantity. They are useful when not the full particulars of the outcomes, but a numerical summary is of interest. This allows to test theories and draw rational conclusions despite of uncertainties. They make it possible to formulate models which then can be compared with reality and might be adjusted afterwards [23].

Mathematically speaking a random variable is a measurable function $X : \Omega \rightarrow \mathbb{R}$. It maps from the sample space to the real numbers and is defined on a probability space $(\Omega, \mathcal{F}, P)$ [16, 47]. For physical applications, particularly this thesis, the requirement of measurability is fulfilled. A formal definition for measurable functions can for example be found in the book [16].

With mapping every observable outcome $\omega \in \Omega$ to a number $X(\omega)$ it is possible to compare vastly different experiments and detect patterns, which is exactly what this work will do [16, 47].

In fact, random variables often are so useful that the sample space Ω can be neglected. The main advantage of random variables is that it is possible to sum, subtract and multiply them, if they are defined on the same probability space. This makes calculation a lot easier and helps describing events with multiple influencing factors.

2.1.3 Types of Probability Distributions

A random variable is fully described by its distribution function [16]. Therefore it is important to take a closer look at them and their connection to the corresponding random variable.

2.1.3.1 Discrete Random Variables

The most important property of discrete random variables is that they can only take values in a countable range [23]. That makes it possible to assign a concrete probability to every outcome $A \in \mathcal{F}$, leading to a discrete probability distribution, which is called probability mass function (PMF). Therefore, a random variable is discrete if and only if the probability distribution is discrete [16].

The probability for an outcome $A \in \mathcal{F}$ can be calculated as

$$P(A) = \sum_{\omega \in A} p(\omega), \tag{2.1}$$

where $p : \Omega \to [0, 1]$ is the probability mass function. P can therefore be obtained from the probability mass function p. For normalization it is important that the probability mass function holds $\sum_{\omega \in \Omega} p(\omega) = 1$ [16].

The binomial distribution, Poisson distribution and the discrete uniform distribution are some well-known discrete probability distributions. A common example for discrete random variables is rolling a dice. For rolling a dice once, the sample space is given as $\Omega = \{1, \ldots, 6\}$, the system of all possible outcomes can be chosen as $\mathcal{F} = \mathcal{P}(\Omega)$. Since the variable is discrete it is possible to name all the possible elementary events $\omega \in \Omega$. The probabilities $P(\omega)$ are defined very easily since $P(\omega) = 1/6 \ \forall \ \omega \in \Omega$, if the dice is fair.

This simple example already shows why the probability distribution is so helpful that it is not really necessary to look at the probability space. The interesting information, i.e. the probability for $\omega = 6$ can easily be obtained from the probability distribution without defining the whole probability space. Is is enough to know the events of interest and the probabilities assigned to them.

In this work durations of certain events in energy system operation are treated as random variables. As the underlying time series is defined in discrete time steps, the duration of an event can only take integer multiples of this fundamental time steps. Hence, this thesis will mostly deal with discrete random variables.

2.1.3.2 Continuous Random Variables

The most important characteristic of continuous variables is that they can take any numerical value in an interval or collection of intervals with an uncountable range. This causes the probability $P(\omega)$ for one specific event $\omega \in \Omega$ to be infinitesimal small, such that a different treatment is needed, compared to discrete random variables.

A continuous random variable is characterized by the cumulative distribution function (CDF), which gives the probability that a random variable X takes a value lower or equal to a real number $x \in \mathbb{R}$. Mathematically the cumulative distribution function for a random variable X is defined as:

$$F : \mathbb{R} \to [0,1]$$
$$F(x) := P(X \leq x).$$

It is called cumulative distribution function since it sums up the probabilities for all different realizations of $X \leq x$.

The most important properties of cumulative distribution functions are:

(i) F is monotonously increasing, meaning for all $s, t \in \mathbb{R}$ with $s \leq t$ the CDF holds $F(s) \leq F(t)$.

(ii) F has a right-hand limit, meaning for every $x \in \mathbb{R}$ the relation $lim_{y \searrow x} F(y) = F(x)$ applies.

(iii) F has a left-hand limit $F(x^-) := lim_{y \nearrow x, y<x} F(y)$, leading to $F(x^-) = P(X < x)$ for every $x \in \mathbb{R}$.

(iv) With that it follows that $P(X \in [a,b]) = F(b) - F(a)$.

(v) Derived from the properties of probability distributions, the relations $lim_{x\to-\infty} F(x) = 0$ and $lim_{x\to\infty} F(x) = 1$ apply.

For applications it is usually enough to know the definition, but a little mathematical background is sometimes helpful [16].

In many cases, it is more instructive to give the probability that a random variable X assumes a value near a given number x, then to quantify the cumulative probability. This probability is given by the probability density function ρ (PDF), which is defined as the derivative of the CDF:

$$\begin{aligned} \rho &: \mathbb{R} \to \mathbb{R}_+ \\ x &\mapsto \rho(x) = \frac{dF(x)}{dx} \,. \end{aligned}$$

The probability that a random variable X lies between the values $a, b \in \mathbb{R}$ is then obtained by integrating the PDF:

$$P(a \leq X \leq b) = \int_a^b \rho(x)\, \mathrm{d}\, x. \tag{2.2}$$

Strictly speaking, PDFs do not always exist. Nevertheless in applications they are often preferred over CDFs, because they are easier to intepret. In particular the quantity $\rho(x)\, \mathrm{d}\, x$ ocurring in the integral (2.2) can be seen as the probability that X takes a value in the infinitesimal interval $[x, x + \mathrm{d}\, x]$.

In contrast the CDF always exists and can be generelized to discrete random variables. It is obtained from the probability mass function via

$$F(x) = \sum_{y \leq x} p(y).$$

Sports give a lot of good examples for continuous random variables. For instance in pole vaulting the jumping height could be understood as a continuous random variable. The probability that an athlete jumps exactly 6 meters high is infinitesimal small. There are very good athletes who can make it approximately that high, but there will always be a decimal place deviating from exactly 6 meters. Whereas the probability that an athlete jumps something between 5.999 and 6.001 can be calculated. With respect to this work, the velocity of the wind is a good example. In theory it can take any positive real number, but even if it was possible to measure without inaccuracies it would never have, lets say, an exact velocity of 20 km/h with no deviating decimal places. This is just because there are infinitely possible velocities. Regardless, wind always has a measurable velocity, because it is inherent to measurement that it gives values with some uncertainty, which is equal to looking for a value in a defined interval.

2.1.3.3 Relation Between Discrete and Continuous

Probability distributions can be discrete, continuous or a mixture of both types. In applications it is often not obvious if the present random variable should be considered discrete or continuous. Since discrete random variables can be approximated by continuous random variables, it can even be helpful to use continuous approximations for variables which obviously are discrete, in favor of a function which is better to calculate.

The general existence of the approximation can intuitively be understood by looking at how to calculate with probability distributions. In the discrete case a concrete probability can be assigned to each event. In the continuous case the probability for one specific event is infinitesimal small, which is why probabilities are calculated with the help of integrals. When comparing equation (2.1) and equation (2.2) it can be seen that for a suitable amount of possible values for the discrete variable it is possible to approximate the sum with the integral [47].

In practice, the link between discrete and continuous distributions can be found with the help of the delta function. For a probability mass function $p(x)$ the corresponding probability density function $\rho(x)$ is given by

$$\rho(x) = \sum_{i=1}^{n} p(x_i)\delta(x - x_i), \tag{2.3}$$

where n is the number of different values the discrete variable can take. While this approach is very helpful in practice, it should be noted that the so defined $\rho(x)$ is not a proper function any more. Strictly speaking, the PDF does not exist, as a proper function, in these cases.

2.1.4 Moments of Probability Distributions

Real-valued random variables have fundamental properties giving information about the shape of the distribution. Starting with the formal and general definition of the k-th moment I will then come to some specific moments which are important for this thesis.

2.1.4.1 Expected Value

The expected value is the first moment of a random variable X. It gives the mean weighted value over all possible outcomes x with probability $p(x)$, respectively the probability density function $\rho(x)$, assuming that it exists [16]. Since the expected value only depends on the probability distribution of X, the formal definition of the expected value should be divided into one definition for the discrete and one definition for the continuous case.

The expected value exists if $\sum_{x\in X(\Omega)} |x| \cdot P(X=x) < \infty$, respectively $\int_\Omega |X(\omega)| \cdot \rho(\omega) \,\mathrm{d}\,\omega < \infty$. To demand the existence might seem a little redundant but it ensures that the summation does not depend on the order of the summands [16].

For a discrete random variable X the expected value is defined as [16]

$$\mathbb{E}(X) := \sum_{i=1}^{\infty} x_i \cdot P(X = x_i) = \sum_{i=1}^{\infty} x_i \cdot p(x_i). \tag{2.4}$$

If the random variable X is continuous with probability density function $\rho(x)$, the expected value is given by [23]

$$\mathbb{E}(X) = \int_{x\in\Omega} x\rho(x) \,\mathrm{d}\,x. \tag{2.5}$$

The expected value is a theoretical construct. The law of large numbers established by Jakob Bernoulli states that the relative frequencies of the possible outcomes $A \in \mathcal{F}$ converge to their probabilities $P(A)$ [47]. From this it can be obtained that the empirical mean converges to the expected value if the random experiment has been repeated sufficiently often and all repetitions have been independent [23]. This link between theory and experiment can be generalized for all k moments.

To calculate with expected values some basic properties are needed. Let X and Y be two random variables with existing expected value and $a, b \in \mathbb{R}$ then

(i) $\mathbb{E}(aX) = a\mathbb{E}(X)$

(ii) $\mathbb{E}(X+Y) = \mathbb{E}(X) + \mathbb{E}(Y)$

(iii) $\mathbb{E}(b) = b$

applies [16].

An easy example of an expected value is rolling a die once. It applies $A = \{1, 2, 3, 4, 5, 6\}$ and $P(A) = 1/6\ \forall A$. Therfore we get $\mathbb{E} = 1/6 \cdot (1 + 2 + 3 + 4 + 5 + 6) = 3.5$.

2.1.4.2 Higher Moments

For $k \in \mathbb{N}$ the k-th absolute moment of a random variable X is defined as

$$m_k = \mathbb{E}\Big(X^k\Big). \tag{2.6}$$

For discrete random variables X with probability mass function $p(x)$, this definition can be rewritten as

$$m_k = \sum_{i=1}^{\infty} x_i^k p(x_i). \tag{2.7}$$

For a continuous random variable X with probability density function $\rho(x)$ the k-th moment of X reads

$$m_k = \int_{-\infty}^{\infty} x^k \rho(x)\, \mathrm{d}\, x. \tag{2.8}$$

To compare the shape of different probability distributions, it is often useful to shift the distribution functions such that their expected values coincide. Accordingly, we can define the k-th central moment. It gives the distribution of a random variable around the expected value and is introduced by a shift in the definition (2.6), leading to

$$c_k = \mathbb{E}\Big((X - \mathbb{E}(X))^k\Big). \tag{2.9}$$

2.1.4.3 Variance

The variance is the second central moment of the real random variable X. It is a measure for the typical quadratic variation of X around the expected value [47]. Mathematically it is the expected value of the deviation of a random variable around the expected value and can therefore be obtained from the first moment $\mathbb{E}(X)$ and the second moment $\mathbb{E}(X^2)$ in the following way [23]

$$\mathrm{Var}(X) = \sigma^2 := \mathbb{E}\Big((X - \mathbb{E}(X))^2\Big) = \mathbb{E}(X^2) - \mathbb{E}(X)^2. \tag{2.10}$$

From this we obtain the standard deviation $\sigma(X) = \sqrt{\mathrm{Var}(X)}$ of a random variable [23].

Given a random variable X and $a, b \in \mathbb{R}$ the most important property is

(i) $\operatorname{Var}(aX + b) = a^2 \operatorname{Var}(X)$, $\forall a, b \in \mathbb{R}$.

For an example we again look a dice. What is the variance? In section 2.1.4.1 we already saw that $\mathbb{E} = 3.5$. $\mathbb{E}(X^2)$ can be calculated as $\mathbb{E}(X^2) = 1/6 \cdot (1^2 + 2^2 + 3^2 + 4^2 + 5^2 + 6^2) = 91/6$. $\operatorname{Var}(X) = \mathbb{E}(X^2) - \big(\mathbb{E}(X)\big)^2 = 35/12 \approx 2.917$, $\sigma(X) = \sqrt{2.917} = 1.71$.

2.1.4.4 Kurtosis

The third central moment scaled by the standard deviation is the skewness of a function and describes the asymmetry of a probability distribution. The skewness will not be deepened further. Instead we will look at the fourth scaled central moment, the kurtosis [16]. It gives the tailedness of a probability distribution. Karl Pearson defined the kurtosis as

$$\kappa(X) = \mathbb{E}\bigg(\Big(\frac{X - \mathbb{E}(X)}{\sigma}\Big)^4\bigg). \tag{2.11}$$

Sometimes a slightly different definition

$$\kappa_{\text{excess}}(X) = \mathbb{E}\bigg(\Big(\frac{X - \mathbb{E}(X)}{\sigma}\Big)^4\bigg) - 3 \tag{2.12}$$

is used. Mostly it is interesting to compare the kurtosis of data to an kurtosis of a specific function. Definition (2.12) compares the tailedness of the respective function to a normal distribution, which has a kurtosis equal to 3. The kurtosis of exponential distributions is 9. The higher the kurtosis, the more extreme values a distribution has. Therefore, the kurtosis gives information about the distribution of extreme values, also called tail extremity. In contrast to persistent notions the kurtosis does not measure "peakedness", since it does not give information about the shape of the peak, but only information about the extremity of tails [63].

A very vivid example of how kurtosis does not measure peakedness is given by Johnson et al. in 1980 [43]. Their figure B. shows 6 functions with the same expected value, variance, skewness and kurtosis but very differed shaped peaks. P.H. Westfall provides an even more impressive example of different shaped curves with the same kurtosis [63]. These figures alone should be enough to see that kurtosis does not give information about the peakedness of a function. Read P.H. Westfall (2014) for more evidence.

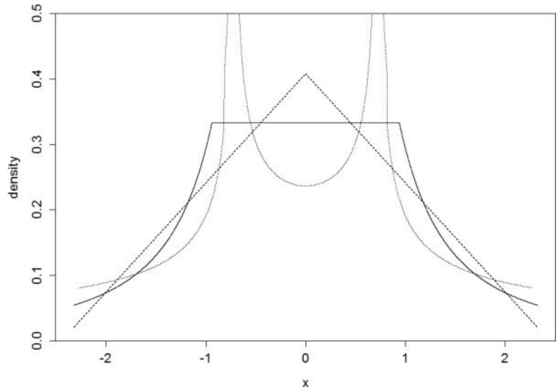

Figure 2.1: Theses very different shaped distributions all have a kurtosis of $\kappa = 2.4$. This figure therefore impressively shows how the kurtosis mainly measures outliers and not the shape of the peak.
(Source: P.H. Westfall, *Kurtosis as Peakedness, 1905–2014. R.I.P.* [63], fig. 2)

2.1.5 Dependence of Random Variables

Independent random variables simplify calculations, yet this simplification is not always valid. In fact, most of the times it is not. Most of the variables analyzed are in some form dependent. To give an example from this work, the velocity of wind in one hour is in some form dependent on the velocity of wind right now and also depends on a whole variety of other random variables.

2.1.5.1 Independence

Mathematically two events $A, B, \in \mathcal{F}$ are called independent if

$$P(A \cap B) = P(A) \cdot P(B). \tag{2.13}$$

Generalized from this a set of random variables $X_1, \dots X_n$ is called independent if all intervals $I_a, \dots, I_n \subset \mathbb{R}$ satisfy

$$P(X_1 \in I_1, \dots, X_n \in I_n) = \prod_{i=1}^{n} P(X_i \in I_i). \tag{2.14}$$

Further a set of random variables is independent if and only if the outcomes of the random variables are independent [16]. This definition will be important when I come to the description of stochastic processes.

2.1.5.2 Conditional Probability

If two random variables X and Y are not independent they will influence each other. Instead of the absolute probability for Y alone, the conditional probability for Y given $x = X$ has to be considered.

The conditional probability for a given x with $P(X = x) > 0$ is defined as

$$p(Y = y|X = x) = \frac{p_{X,Y}(x, y)}{p_X(x)} \tag{2.15}$$

and is often abbreviated as $p(y|x)$ [16]. This definition will help when taking a closer look at stochastic processes.

2.1.5.3 Covariance

The covariance is a measure for the monotone correlation of two random variables with a joint probability distribution. It measures how well the correlation of two random variables can be described by a linear function [16].

For two random variables X and Y the covariance is defined as

$$\text{Cov}(X, Y) = \mathbb{E}([X - \mathbb{E}(X)] \cdot [Y - \mathbb{E}(Y)]) = \mathbb{E}(X \cdot Y) - \mathbb{E}(X) \cdot \mathbb{E}(Y) \tag{2.16}$$

and only depends on the joint probability distribution of X and Y.

Positive covariance of two random variables X and Y indicates that higher values of one variable correspond with high values of the other variable, meaning two variables tend to show the same behavior. Negative covariance indicates that higher values of one variable correspond with low values of the other variable, meaning two variables tend to show opposite behavior. If $\text{Cov}(X, Y) = 0$, the random variables X and Y are uncorrelated. Independent random variables always are uncorrelated. It is important to note that covariance is not the same as correlation since a positive covariance only indicates whether two variables show the same behavior. It does not describe whether two variables influence each other [47].

Nevertheless the covariance is hard to interpret since it is not normalized which makes comparison impossible. The **Correlation Coefficient** is a normalized version of the covariance and is defined as [23]

$$r_{X,Y} = r(X,Y) := \frac{\mathrm{Cov}(X,Y)}{\sqrt{\mathrm{Var}(X) \cdot \mathrm{Var}(Y)}}. \tag{2.17}$$

The correlation coefficient only takes values between -1 and $+1$. If $r_{X,Y} = +1$ or $r_{X,Y} = -1$ the random variables X and Y are associated by $Y = c \cdot X + d$, where $c, d \in \mathbb{R}$. The closer $r_{X,Y}$ is to $+1$ or -1, the more the values $(X(\omega), Y(\omega))$ follow a straight line [47].

Moreover covariance and the correlation coefficient can be used to describe the correlation of two different values of one time series. For this purpose they are often called autocovariance, receptively autocorrelation [14].

In section 2.3 measures for the correlation between two random variables, used in this thesis, will be given.

2.2 Stochastic Processes

Stochastic processes describe systems that change randomly over time [14]. Mathematically a stochastic process $\{X(t) : t \in T\}$ is a sequence of chronologically ordered random variables. The variables $X(t)$ take values in some set $\mathcal{X}$, called the state space and T is called the index set and for this work will be thought of as time [61].

In that sense a time series is a set of observations $X(t)$, of the random variable X, where each observation is being recorded at a specific time t. It can be distinguished between continuous-time time series when observations are recorded continuously over some time interval and discrete-time time series where the observations are made at discrete times [9]. Furthermore, it can be distinguished whether the state space $\mathcal{X}$ is discrete (referred to as "value-discrete") or continuous ("value-continuous").

Since the velocities of wind are recorded at discrete times, the electricity prices only change at discrete times and the power generation, respectively the load, is also only given for discrete intervals, all time series appearing in this work can be thought of as discrete.

An example for the time series of a stochastic process could be $\mathcal{X} = \{\text{calm, windy, stormy}\}$ with a discrete-time time series $\{\text{calm, calm, windy, windy, stormy, windy}\}$. This basic idea will be used for analyzing data in this work.

2.2.1 Markov Chains

Markov chains, named after the Russian mathematician Andrey Markov, are a model of a stochastic process with dependend random variables. It models a particularly simple dependence and is used to analyze a variety of scientific data. For a given time series $x_0, \ldots, x_n$ the outcome x_{n+1} of the next time step only depends on the present value x_n of the random variable and not the ones before that. This "short memory" property is called Markov property and is crucial for Markov chains. For the sake of simplicity it is furthermore required that the process is time-invariant [7, 23]. The Markov property can be formulated and analyzed for both value-continuous and value-discrete stochastic processes. However, we will restrict ourselves to value-discrete processes, which are much easier to handle in practice. To create a countable set of possible values out of a continuous space "binning" can be used [7].

Markov chains can either be represented by a transition matrix $\boldsymbol{P}$ with

$$\boldsymbol{P}(x, y) = P(X_{t_{n+1}} = y | X_{t_n} = x) \tag{2.18}$$

meaning each entry $\boldsymbol{P}(x, y)$ contains the probability that the system would jump from state $X = x$ to state $X = y$ or can be visualized as a graph giving the probability to jump from one realization to another [23]. In applications the identification of the transition probabilities takes the most effort [7].

The powers of the transition matrix $\boldsymbol{P}$ play an important role in describing the evolution of Markov processes, because $\boldsymbol{P}^n$ gives the probability that the system with a defined starting point is in a certain state after n time steps, which is often the ultimate goal of creating Markov chains [7, 23].

An example for a Markov chain is the random walk, in which at each time step a person randomly takes a step either to the left or to the right. As time progresses, the location of the person is the random variable of interest [7].

More information about the properties of Markov chains can be e.g. found in the text book [7].

2.2.1.1 Telegraph Noise

A telegraph process is an example for a Markov process with two district possible values $X_t \in \{0, 1\}$. It is used to model Telegraph noise, also known as burst noise or bistable noise. It originates from transitions between two discrete voltage or current levels at random and at unpredictable times, leading to popcorn popping like noises, which is why it is also called popcorn noise. This fluctuations might be related to electrons switching energy levels since it reduces if the device area is scaled down [52].

The transition probabilities can be represented by

$$\begin{aligned} P(X_t = 1 | X_{t-1} = 0) &= \omega \\ P(X_t = 0 | X_{t-1} = 0) &= 1 - \omega \\ P(X_t = 1 | X_{t-1} = 1) &= 1 - \omega \\ P(X_t = 0 | X_{t-1} = 1) &= \omega, \end{aligned}$$

leading to the transition matrix

$$\boldsymbol{P} = \begin{pmatrix} 1-\omega & \omega \\ \omega & 1-\omega \end{pmatrix}, \tag{2.19}$$

which can also be represented by a transition graph (cf. fig. 2.2). This concept can be generalized by assigning different transition probabilities for the different states.

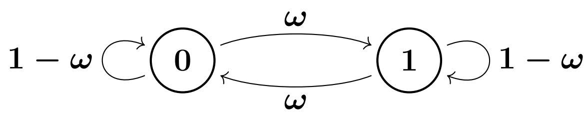

Figure 2.2: Transition graph for a two state Telegraph noise.

With respect to this work state 0 could be interpreted as having to little or too much wind for wind power generation and state 1 could mean the velocity of wind being in a certain range so wind power generation is doable.

Although it is not possible to predict when exactly the transition between the states will happen, it is possible to define the waiting time distribution for this process which will be done in section 2.2.2.1.

2.2.2 Waiting Time

Waiting time, or better to say waiting time distributions, can give important information about stochastic systems. In general, a waiting time distribution is derived from a random variable T which measures how many time steps τ (for discrete stochastic processes), respectively how much time (for continuous processes), lie between two events. A term often used in this context is persistence, meaning the time the system stays in a specific state or a specific set/range of states.

Since the underlying process is stochastic T will take different values τ each time it measures the waiting time between the events of interest. A histogram of T makes it possible to see how the waiting times are distributed stochastically.

Waiting times can for example be used to describe how many tries it would take to roll a Yahtzee without having to re-roll the dice, to measure the quality of an operational amplifier by determining the waiting time distribution between two Telegraph noises or with regard to this work the time in which electricity prices are below a certain limit.

2.2.2.1 Waiting Time Distribution for the Telegraph Noise

For the example of a Telegraph noise with two possible states, the random variable T would measure how many time steps τ the system stays in state 0, meaning how much time no burst noise occurs, leading to $T = \tau$.

$$1 \rightarrow \underbrace{0 \rightarrow 0 \rightarrow 0 \rightarrow 0 \rightarrow \ldots \rightarrow 0 \rightarrow 0}_{\tau \text{ time steps}} \rightarrow 1$$

Of course T has to be determined multiple times to get a waiting time distribution, since the burst noises occur at unpredictable times. The probability that the system stays exactly τ time steps in state 0 is given by

$$P(T = \tau) = P(X_{\tau+1} = 1, X_\tau = 0, \ldots, X_1 = 0 | X_0 = 1).$$

Therefore the probability can be written as

$$P(T = \tau) = \omega(1-\omega)^\tau = \omega e^{\ln((1-\omega)^\tau)} = \omega e^{\tau \ln(1-\omega)} \sim e^{-\tau/\tau_0}$$

with $\tau_0 = -1/\ln(1-\omega)$, which illustrates how the probability decays exponentially with τ.

For the example of Telegraph noises with multiple possible states, the random variable T could for example measure how many time steps τ the system stays in a state $X \leq n$. The probability for this is given by

$$P(T = \tau) = P(X_{\tau+1} > n, X_\tau \leq n, \dots, X_1 \leq n | X_0 > n)$$

and is not necessarily exponentially distributed.

This simple examples are very close to the waiting times which will be calculated for this work, since I will calculate the waiting time for electricity price being below or above a certain limit.

2.2.2.2 Waiting Time Distribution for Poisson Processes

A counting process $\{N(t), t \geq 0\}$ counts the number of events $N(t)$ of a stochastic process that have occurred up to time t. The Poisson process is a special counting process. A Poisson process with rate $\lambda,\ \lambda > 0$ has the following properties:

(i) $N(0) = 0$, meaning the counting of events begins at time $t = 0$.

(ii) The process has independent increments, meaning that the number of events in one interval is independent of the number of events in any other disjoint interval.

(iii) The number of events in any interval of length Δt is Poisson distributed with mean λt, leading to

$$P_n(\Delta t) = P((N(t + \Delta t) - N(t)) = n) = e^{-\lambda \cdot \Delta t} \frac{(\lambda \Delta t)^n}{n!} \tag{2.20}$$

for $n \in \mathbb{N}$. The number of events therefore only depends on the length of the time interval.

From condition (iii) it follows that the expected value for the number of events in an interval of length Δt is given by

$$\mathbb{E}(N(\Delta t)) = \lambda \Delta t. \tag{2.21}$$

Which explains why λ is called the rate of the process. Further the variance is given by

$$\mathrm{Var}(N(\Delta t)) = \lambda \Delta t. \tag{2.22}$$

For a Poisson process the random variable T_n measures the time between the $(n-1)$-st and the n-th event, hence the waiting time between two events. To get the distribution of T_n we note that $T_1 > t$ applies if and only if no event occurs in the interval $[0, t]$, leading to

$$P(T_1 > t) = P(N(t) = n = 0) = e^{-\lambda t}, \tag{2.23}$$

with the use of equation (2.20). Because the different values of T_n are independent and identically distributed this leads to the fact that the waiting times are exponentially distributed with a mean of $1/\lambda$. Hence the Poisson process is a counting process with exponentially distributed waiting times between two events [54]. More information on the Poisson process, derivations and the respective waiting times can be found in book [54].

2.3 Empiric Data Analysis

Statistic analyses data with the help of stochastic models. It extracts essential quantities out of empiric data with the help of suitable statistical models [23]. Finding an appropriate model often is neither obvious nor is there only one correct answer. The goal is to find the best fitting model for finding patterns in stochastic processes [23]. Estimators help with a strategy for finding suitable statistic models.

2.3.1 Estimators

An estimator helps estimating a given but unknown quantity based on empiric data. For a value θ the estimator often is written as $\hat{\theta}$. It is used if the underlying probability distribution is unknown or unclear. This is true for almost all empiric data, which is why estimators are very important for data analysis. It is crucial to note that the value of an estimator depends on the given sample. Which is why it is important to carefully choose the used estimator and to calculate errors for the estimator as a quality measure.

There are several types of estimators for different purposes and even different estimators for the same property [23]. In the following I will concentrate on maximum likelihood estimation.

2.3.1.1 Maximum Likelihood Estimation

Up until now we always had a situation with a given probability distribution and could get the probability for a certain outcome out of it. Now we have the opposite situation. We are given a sample set and the question is which parameter, for a given distribution, makes the observed data most likely. Since there are stochastic deviations in the data, is it very unlikely to get exactly the same quantities out of one sample as one would get when looking at the whole set of outcomes. Therefore it is important to find an estimator which most likely fits to the given sample, called the maximum likelihood estimator. It is a parametric estimator and gives the parameter $\hat{\theta}$ for which the empiric data x is the likeliest. In the discrete case the function $L_x = P_\theta(x)$ is called the likelihood function. Therefore the maximum likelihood estimator $\hat{\theta}(x)$ for an unknown parameter θ can be determined with

$$L_x(\hat{\theta}) = \sup\{L_x(\theta) : \theta \in \Theta\}. \tag{2.24}$$

In other words: the maximum likelihood estimator $\hat{\theta}(x)$ takes the value for which the given sample is most likely. For the continuous case the likelihood function is defined as

$$L_x(\theta) = \rho(x, \theta), \tag{2.25}$$

with ρ being the probability density function.

In many elementary cases, the maximum likelihood estimator can explicitly be obtained by calculating the roots of the derivative of the likelihood function with respect to the parameter θ. In practice, these calculations are often simplified by using the log-likelihood function

$$\mathcal{L}_x(\theta) = \ln(L_x(\theta)). \tag{2.26}$$

Because of the monotony of the logarithm, it reaches its supremum for the same value as the likelihood function.

In more complex applications, the condition $\frac{\mathrm{d}}{\mathrm{d}\,\theta} L_x(\theta) = 0$ does not always have an explicit solution, meaning a maximum of the function does not exist, only a supremum. In this cases $\hat{\theta}(x)$ can be approximated.

To get a good estimation it is important that the empirical sample x contains enough independent observations. Further the maximum likelihood estimator demands that the type of the probability distribution for the present situation is given. So the maximum likelihood estimator gives the best fitting value for a given probability distribution but it does not give any information if the chosen probability distribution is right. Therefore the quality of an estimator highly depends on the suitability of the chosen model [47].

For the **Exponential Distribtion** with a parameter $\lambda > 0$ the density function is given by $\rho(x) = \lambda e^{-\lambda x}$. The maximum likelihood estimator $\hat{\lambda}(x)$ for a given sample set $x = \{x_1, x_2, \dots x_n\}$, where the x_i are independent, can be calculated as follows

$$\begin{aligned} L_x(\lambda) =& \prod_{i=1}^{n} \rho(x_i) = \prod_{i=1}^{n} \lambda e^{-\lambda x_i} \\ =& \lambda^n e^{-\lambda \sum_{i=1}^{n} x_i}. \end{aligned}$$

Using the log-likelihood function makes it easier here

$$\begin{aligned} \mathcal{L}(\lambda, x) = \ln(L(\lambda, x)) &= \ln\left(\lambda^n e^{-\lambda \sum_{i=1}^{n} x_i}\right) = \ln(\lambda^n) + \ln\left(e^{-\lambda \sum_{i=1}^{n} x_i}\right) \\ &= n \cdot \ln(\lambda) - \lambda \sum_{i=1}^{n} x_i. \end{aligned}$$

The maximum likelihood estimator can be found from the roots of the derivative

$$\begin{aligned} \frac{\mathrm{d}}{\mathrm{d}\,\lambda}\mathcal{L} &= \frac{\mathrm{d}}{\mathrm{d}\,\lambda}\left(n \cdot \ln(\lambda) - \lambda \sum_{i=1}^{n} x_i\right) \\ &= n \cdot \frac{1}{\lambda} - \sum_{i=1}^{n} x_i \overset{!}{=} 0 \\ \Leftrightarrow \qquad \frac{n}{\lambda} &= \sum_{i=1}^{n} x_i \\ \Leftrightarrow \qquad \hat{\lambda} &= \frac{n}{\sum_{i=1}^{n} x_i} = \frac{1}{\bar{x}}. \end{aligned}$$

Hence the maximum likelihood estimator of the parameter λ is the inverse of the sample mean $\bar{x}$.

2.3.1.2 Bias of Empirical Estimators

Measured data is always finite. Computing statistical quantities and estimators from small data sets can cause errors, which must be carefully reflected when interpreting the results. In particular, empirical results may not only be subject to uncertainties, but also to a systematical bias.

A common example is the estimation of the variance. Given a data set $x = x_1, \dots x_n$ of a random variable X, following equation (2.10), the variance should be estimated as

$$\mathrm{Var}(X) = \frac{1}{n} \sum_{i=1}^{n} (x_i - \mathbb{E}(X))^2, \tag{2.27}$$

but the true expected value is unknown. By replacing the theoretical expected value $\mathbb{E}(X)$ with the sample mean $\bar{x}$, we obtain

$$S^2_{\text{biased}} = \frac{1}{n} \sum_{i=1}^{n} (x_i - \bar{x})^2, \tag{2.28}$$

but this formula generally underestimates the empiric variance S^2, because the sample mean $\bar{x}$ is a minimizer of the expression S^2_{biased}. Hence, replacing the theoretical expected value with the empiric mean can only decrease the value of the variance. The correct estimator for the sample variance takes that bias into account and is given by

$$S^2 = \frac{1}{n-1} \sum_{i=1}^{n} (x_i - \bar{x})^2. \tag{2.29}$$

The difference between these estimators vanishes with large sample sizes n, which is one of the reasons why large data sets are needed to provide good evidence.

Similarly, the sample excess kurtosis, following equation (2.12), given by

$$\kappa_{\text{excess, biased}} = \frac{1}{n} \frac{\sum_{i=1}^{n} (x_i - \bar{x})^4}{S^4} - 3 \tag{2.30}$$

is a biased estimator. If the random variable X is normally distributed, the revised formula

$$\kappa_{\text{excess, normal}} = \frac{(n+1)n}{(n-1)(n-2)(n-3)} \frac{\sum_{i=1}^{n} (x_i - \bar{x})^4}{S^4} - 3 \frac{(n-1)^2}{(n-2)(n-3)} \tag{2.31}$$

provides an unbiased estimator. This expression is used in most statistical software packages [42], but for distributions other than the normal distribution, the correction is not sufficient to remove the bias. For the exponential distribution both equation (2.30) and (2.31) systematically underestimate the kurtosis [8]. Therefore, the kurtoses κ_{excess} for small samples, drawn from an exponential distribution, are typically below the true value $\kappa_{\text{excess}} = 6$.

2.3.2 Correlation Measures

Detecting dependence between different random variables is of central importance in statistical analysis and modeling. But correlation measures must be interpreted with great care. Statistically dependent random variables X and Y can still have a vanishing correlation coefficient and non-vanishing correlation coefficients only reveal a statistical, but not necessarily a causal relation. Nevertheless, correlations measures can be extremely useful to direct further research. In the following I will introduce the correlation measures used in chapter 4 of this thesis.

2.3.2.1 Linear-fit

A linear fit, also called linear regression, is the simplest way of describing the dependence between a random variable and an explanatory variable, which can be adjusted to any arbitrary value in a physical possible range. A linear fit can therefore be done if the value of the respective random variable does not only depend on chance but also on the value of an explanatory variable in a linear way[1].

If it can be assumed that a scalar random variable depends linearly on an explanatory variable, a linear regression can be made and the relation is represented by

$$Y = \alpha + \beta x + \epsilon, \tag{2.32}$$

where Y is the outcome of the experiment, x is the value of the explanatory variable and ϵ is an unbiased ($\mu = 0$) normal distributed random variable, representing random observational errors with unknown coefficients. It represents everything that cannot be explicitly measured during the experiment. $\alpha, \beta \in \mathbb{R}$ are the regression coefficients which need to be determined [23]. For this purpose the experiment is repeated n times for different values of the explanatory variable x, leading to the relation

$$y_i = \alpha + \beta x_i + \epsilon_i \tag{2.33}$$

[1] Linear regression can also be done if the dependence between the random variable and the explanatory variable cannot be directly described as a line but can be linearized. Meaning, the values Y are not plotted against x but against a function depending on x or the other way around. For example if the interrelation $y = ax^2 + b$ is assumed the values of Y will be plotted against values $f(x) = x^2$ so the linear dependency $y = \alpha + \beta f(x) + \epsilon$ can be estimated. Another example is the use of the logarithm. If the interrelation $y = \alpha e^{\beta x}$ is assumed a linear relation $f(y) = \ln(\alpha) + \beta x$ with $f(y) = \ln(y)$ can be estimated.

for one data point (x_i, y_i). When plotting the data points (x_i, y_i) one can see that, because ϵ_i varies, the data points do not lie on a straight line but scatter around it.

The practical problem lies in the estimation of the regression coefficients α and β, which can be done with the help of the maximum likelihood estimator.

2.3.2.2 Pearson Correlation Coefficient

The Pearson correlation coefficient, sometimes called Pearson's r, is a parametric test measuring the linear empiric correlation between two observed random variables x and y with the data sets $x = x_1, \dots x_n$ and $y = y_1, \dots y_n$. It is calculated analog to the correlation coefficient in section 2.1.5.3 but instead of the theoretical moments the empiric mean and the empiric variance are used, leading to [7]

$$r_{x,y} = \frac{\sum_{i=1}^{n}(x_i - \bar{x}) \cdot (y_i - \bar{y})}{\sqrt{\sum_{i=1}^{n}(x_i - \bar{x})^2} \cdot \sqrt{\sum_{i=1}^{n}(y_i - \bar{y})^2}}. \tag{2.34}$$

One problem is that the Pearson correlation coefficient is very sensitive to outliers and can therefore lead to a misleading impression, hence is not robust [17].

2.3.2.3 Spearman's ρ

Spearman's ρ is a non-parametric measure for the correlation of the ranking of two empiric random variables and makes no assumptions about the underlying probability distribution [35]. The rank of the values of an observed random variable x is obtained by sorting the data set $x = x_1, \dots x_n$ into ascending (or descending) order and replacing the values by their rank. For example the finish times 17.4, 12.8 and 13.6 of a 100-metre dash will be assigned to the ranks 3,1 and 2.

Spearman's ρ is defined as the Pearson correlation coefficient equation (2.34) between the rank of the variables [56], leading to

$$\rho_s = r_{rank(x),rank(y)} = \frac{\mathrm{Cov}(rank(x), rank(y))}{\sqrt{\mathrm{Var}(rank(x)) \cdot \mathrm{Var}(rank(y))}}. \tag{2.35}$$

It can take values from -1 to $+1$ where both extremes mean that the relation of the two variables can be perfectly described by a monotone function. If a ranking of the observed data is possible, Spearman's ρ can be calculated.

Spearman's ρ measures how well the correlation between the ranks of two random variables can be described as a monotonic function. The shape of the function does not matter, it only matters if it is monotone. This is the biggest difference to the Pearson correlation coefficient, which is a measure for linear correlation.

2.3.2.4 Kendall's τ

Kendall's τ, also known as Kendall's rank correlation coefficient, is a non-parametric measure for the rank correlation of two variables, alike the Spearman's ρ. It can be calculated as

$$\tau_B = \frac{n_C - n_D}{\sqrt{(n_C + n_D + n_{T_X}) \cdot (n_C + n_D + n_{T_Y})}}, \tag{2.36}$$

where n_C counts the number of concordant data pairs and n_D counts the discordant pairs. Concordant means that either $x_i \leq x_j$ and $y_i \leq y_j$ or $x_i \geq x_j$ and $y_i \geq y_j$ are true. Discordant is defined as either $x_i \leq x_j$ and $y_i \geq y_j$ or $x_i \geq x_j$ and $y_i \leq y_j$. n_{T_x} and n_{T_y} represent the ties in the x- and y-values. n_{T_x} counts how many x-values coincide, so does n_{T_y} for the y-values respectively [45][2].

Kendall's τ is normalized and takes values between -1 and $+1$. Higher values indicate that two variables show rather similar ranks, meaning if the probability for $y_i \leq y_j$ given $x_i \leq x_j$ increases, so does Kendall's τ. Lower values indicate that two variables show dissimilar ranks, meaning it is more likely that $y_i \leq y_j$ given $x_i \geq x_j$.

Compared to the Spearmans ρ, Kendall's τ is more sensitive to outliers, because it does not take the rank itself but the difference of two values. Further Kendall's τ assesses a linear relationship between two variables whereas Spearman's ρ reckons the relations is monotonic, independent of the specific function.

[2] Another definition of Kendall's correlation coefficient is $\tau_A = \frac{n_C - n_D}{n(n-1)/2}$, which does not account that data points can be equal. A third definition is $\tau_C = \frac{2(n_C - n_D)}{n^2(m-1)/m}$ with $m = \min\{\text{Number of possible } x\text{-values, Number of possible } y\text{-values}\}$. It is best used if the number of possible x- and y-values is inequal [45].

3 Renewable Energy Systems

Anthropogenic climate change is the central challenge for today's human civilization. Since industrialization human activity added a substantial amount of greenhouse gases to the atmosphere. The level of CO_2, the most common greenhouse gas, in the atmosphere has never been higher in the last 2.1 million years and the yearly emissions keep increasing [38]. This is problematic as greenhouse gases in the atmosphere detain heat radiation from the sun to be fully emitted back to space, which leads to a thermal disequilibrium, since the Earth absorbs more energy than it emits. This effect is called the greenhouse effect[1].

In general, the greenhouse effect is required to make Earth habitable. Without it the mean temperature would be about 33°C lower [36] but as the concentration of greenhouse gases in the atmosphere gets higher and higher overheating becomes a problem. The global mean temperature has already risen by approximately 1°C above the pre-industrial level, before 1750, increasing at around 0.2°C per decade [40]. Effects that can already be observed are changes in the global water cycle, reduction in snow and ice, more frequent climate extremes, acidification of the ocean and the rise of mean see level due to thermal expansion and shrinking glaciers, to name only a few [29, 38]. Even though individual events cannot directly be ascribed to human influenced climate change, it is very likely that this has been the dominant cause [38][2]. The effects and their consequences are expected to get more extreme, the more the temperature rises. For further information on this topic the reports of the Intergovernmental Panel of Climate Change (IPCC) give detailed and accessible overviews on different scenarios.

---

1 The greenhouse effect is caused by sun radiation entering the atmosphere, then being absorbed by the Earth's surface, where conversion leads to longer wavelengths which then will be emitted to the atmosphere. These longer wavelengths partly get absorbed by greenhouse gases in the atmosphere and do not make their way back to space [36].

2 In the IPCC report from 2013 (Page 18, Figure SPM.6) models which only consider natural forcings and models which also consider human influence are compared. It impressively shows that models which also consider human influence are a lot closer to the observations [38].

To mitigate climate change substantial and sustained reduction of greenhouse gas emissions are required before tipping points are reached [38]. The latest report of the IPCC states that it still is possible to limit global warming to 1.5°C, but it would require "unprecedented transitions in all aspects of society" [40]. Every bit of warming matters, so rapid progress is needed [40].

Many countries have already taken actions against climate change, but there is still a lot to do, as the world wide CO_2 emissions are still rising [38]. The Paris Agreement, concluded in 2015, aims to keep the global temperature rise well below 2°C and therefore demands an extensive decarbonization, since the emission of greenhouse gases is the most important determinant of future climate change [59].

World wide around 65% of all greenhouse gas emissions is CO_2 of fossil fuel and industrial processes [39]. In Germany the percentage is even higher and lies around 84% [3]. This includes but is not limited to power generation and transportation. Therefore even though a transition to a fully renewable power system is not enough, for the emissions to fall to zero, it is a key starting point for other transitions to follow. Electricity can for example be used to substitute fuels in heating, transport and industry. This illustrates how the expansion of renewable energy sources is a major strategy for achieving the climate goals [50].

Germany aims to reduce its greenhouse gas emissions by 80-95% until 2050. Renewable energy sources should make substantial contributions [19] and should be the first step to mitigate global warming world wide [39]. The EU directive 2009/28/EG details concrete goals for the percentage of renewable energy in the gross final energy consumption[3] in 2020. For Germany the percentage should be at least at 18% [21]. In 2018 it reached 16.7%. If only power consumption is considered it has been around 37.8% [4]. So to reach the goals of zero emission there is still a lot to do.

[3] Gross final energy consumption includes all energy consumption of the transport sector, industries, service industries, agriculture, forestry, fishery and households. Further it includes all electricity and thermal losses due to power and heat generation, as well as the losses due to distribution and transmission. Therefore, for increasing the share of renewable energy in the gross energy consumption it is not only possible to increase the quantity of power from renewable sources, but it is also possible to enhance the efficiency of conventional power plants. In the EU directive 2009/28/EG this opportunity is explicitly specified [21].

3.1 Development of Renewable Energy Sources

World wide the share of renewable energy is growing every year. In 2018 it has been at around 26% [33]. Countries like Iceland (100%), Norway (97%), Costa Rica (93%) and Brazil (76%) show a remarkably higher share, mostly based on hydropower [48].

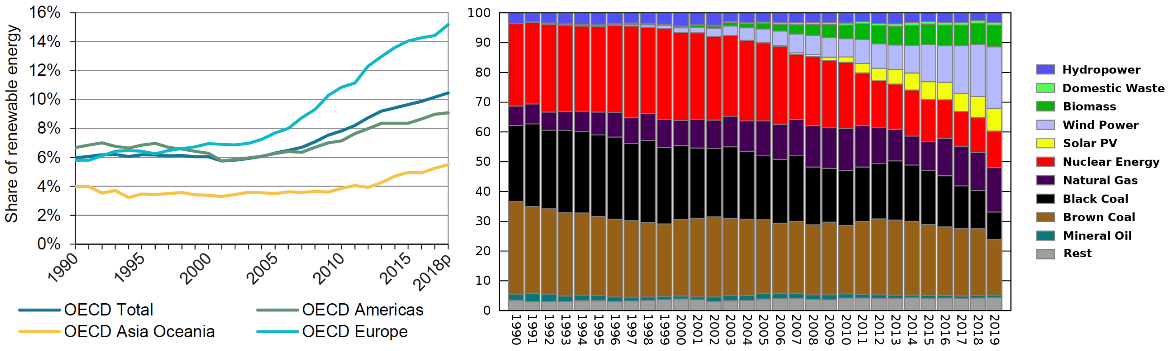

(a) (b)

Figure 3.1: **(a)** Since 1990 the share of renewable energy in OECD countries increased in all regions. **(b)** In Germany the share of renewable energy is even higher. Nevertheless, conventional power plants still have the largest share.
(Source: **(a)** IEA, *Renewables information: Overview* [32], p. 7, fig. 11 and 12. All rights reserved. **(b)** https://commons.wikimedia.org/wiki/File:Energiemix_Deutschland.svg, User: Tkarcher, (CC BY-SA 3.0), visited: 15.07.2020. The original is modified by translating the description into English and leaving out the header.)

Although the percentage increase of renewable energy sources world wide is higher than of any other energy source, it does not make up for the growth of energy demand [53]. To say it in other words, the demand is growing faster than the availability of renewable energy. This makes it even more important to study beneficial as well as, hampering influencing, factors and develop the respective technologies to foster the installation of renewable power plants world wide, as they are the center of the transition to a more sustainable energy system.

In Germany the share of renewable energy in the power supply has risen over the last decades and totalled 37.8% in 2018 [4] and is planned to be further increased [4, 5, 19]. The most promising technologies to reach a high share in Germany are wind power and solar photovoltaic [19, 37, 41, 62]. Figure 3.1b shows the German development of renewable energy sources over the last decades. Especially the development and the high share of wind power is remarkable.

How will renewable energy sources develop? How will the electricity mix be in a few years? This will be determined by newly commissioned power plants, which will depend on the enhancements of the respective technologies and their cost effectiveness. Besides the costs, the handling of difficulties, described in section 3.4, will crucially determine future development. Therefore research on all corresponding topics is necessary for a fast and reliable transition to a highly renewable energy system according to climate goals[4].

3.2 Renewable Energy Technologies

Renewable energy is a fundamental starting point for mitigating climate change. There are a lot of different technologies to achieve the goal of a highly renewable energy system. It is important to examine the potential of each technology based on geographical conditions as well as technical, social and financial implications. With knowledge of these factors different scenarios can be created, to make the best possible use of the technologies and combine them optimally. The primary considered technologies for Germany are hydropower, geothermal energy, biomass energy, concentrated solar power, photovoltaic and wind power.

Hydropower plays an important role in a lot of countries with a high share of renewable energy, like Iceland, Norway and Costa Rica [48]. It has been used for decades, as it has been an inexpensive way to generate renewable energy. Between 2010 and 2018 most hydropower cost less than the cheapest fossil fuel alternative [41]. However this technology is driven by natural rainfall and geographic topology [48] and can cause major environmental impacts [15]. Most good sites for large hydropower plants have already been developed around the world [48], so the potential for future development in Germany is very limited.

Geothermal power generation is independent of weather and time and could therefore theoretically be used for the base load, since it is constantly available. For example, in Iceland geothermal power is a key technology for the energy system [48]. Today's geothermal power plants are hydrothermal systems, which operate with hot water aquifers, water-bearing formations, under the Earth's surface. Equivalent to hydropower, certain

[4] A full report on scenarios with different shares of renewable energy and different shares of the possible technologies for Germany can be found in the analysis *Flexibilitätskonzepte für die Stromversorgung 2050* [19]. Abb. 2 on p. 21 gives an overview about the considered scenarios examined in the report. An analysis of the global development can for example be found in the IEA reports *Renewables 2019* [33] and *World Energy Outlook 2019* [34].

geological requirements are needed [19]. In Germany the share of geothermal power is very low and it is relatively expensive, but in the future it could be used to compensate fluctuations in the generation of other renewable energy sources [19].

Energy generation from biomass is also flexibly applicable and may furthermore be cheaper than geothermal power generation, but its potential highly depends on the availability of biomass. The cultivation of energy crop competes with agricultural land for food production, so the extent of bio energy must be weighed out carefully. In a lot of renewable energy scenarios for Germany it is used for compensating fluctuations in other renewable energy sources. The percentage of bio energy can be further reduced, the more wind and photovoltaic energy is produced, in combination with sufficient storage technologies [19].

Concentrated solar power (CSP) is predictable and adjustable, since thermal energy can easily be stored, e.g. in storage tanks with hot melted salt. Unfortunately solar thermal power plants can only process direct sunlight, which limits the appropriate locations. Hence for Germany power lines from countries around the mediterranean sea would be the only cost-efficient option to use CSP [19].

Solar photovoltaic is a key technology for all scenarios of highly renewable energy systems in Germany. It is economical and socially accepted in all regions of Germany [19] and could contribute a lot to a renewable energy system, even though the potential is rather low compared to other countries (cf. fig. A.1a). Nevertheless photovoltaic power plants only generate power during daytime [65], so photovoltaic power generation has to be combined with storage technologies and other renewable energy sources, like wind power.

Wind power is essential to the transition to a highly renewable energy system in Germany [19, 48, 50, 62]. Wind power has a remarkably high potential and could generate enough electricity to meet the global demand [31, 39]. Furthermore its costs can compete with fossil fuels [41]. Especially offshore wind power has a remarkably high potential which still could be developed to match the electricity demand [31] (cf. fig. A.1b).

Compared to onshore wind power, offshore wind power has a higher electricity generation per square meter, since the wind blows faster and steadier. Furthermore, location issues due to visual and noise impacts are less, which results in a higher public acceptance [30]. Until 2030 the offshore wind power capacities in Germany should be increased to 20GW [5]. However wind power is highly dependent on weather, so to design a reliable highly renewable power system the variability of wind needs to be well understood.

3.3 Costs of Renewable Power Plants

Important for the commission of new renewable power plants is their cost effectiveness. In most parts of the world renewable power became the lowest-cost source of all newly commissioned power plants. Especially the costs for solar and wind technologies continue falling and expectations about future cost reductions are continually beaten by lower values as new data becomes available.

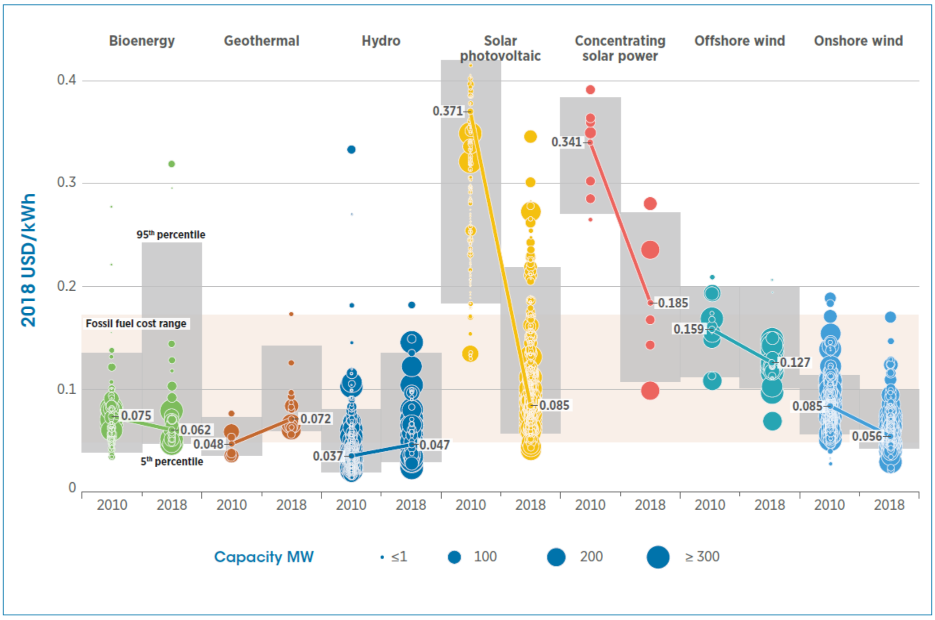

Figure 3.2: This data is plotted for the year of commissioning. The center of each circle represents the costs of the project, the diameter stands for the size of the project. The single light brown band represents the cost range of fossil fuels.
(Source: IRENA, *Renewable Power Generation Costs in 2018* [41], p. 12, fig. S.1)

Since 2010 the global weighted-average cost of electricity from biomass, geothermal, hydropower and onshore wind projects have all been within the range of fossil fuel power generation. In 2018 the costs have been at the lower-end of the fossil fuel cost range [41]. From 2000 to 2013 the costs for the production of photovoltaic modules dropped by 90% [19], consequential solar photovoltaic is also at the lower-end of the fossil fuel cost range since 2014 [41][5]. These technologies can therefore compete with fossil fuels even

[5] The data stems from the IRENA Renewable Cost Database which contains cost and performance data for around 17 000 renewable power generation projects with a total capacity of around 1 700GW. It has data on around half of all renewable power generation projects commissioned by the end of 2018.

without financial support [41]. More detailed information about the costs of renewable energy sources can be found in the IRENA report *Renewable Power Generation Costs in 2018* [41].

3.4 Challenges of Renewable Energy Systems

Photovoltaic and wind power will be the major contributors to a highly renewable power system in Germany. They have a high potential, are available at scale and are cost competitive (cf. sec. 3.3) [19, 30, 41, 48], but they also come with difficulties. The central challenges are the need for long-distance transmissions, the connection of renewable energy sources to the power grid and of course the variability of renewable energy sources. Therefore, the optimal design of networks, dynamical stability of complex networks and the fluctuations in power generation are fundamental research topics with growing importance.

Long-distance transmission becomes necessary because renewable energy, especially wind power, is often generated at profitable locations, which can be far away from the consumers [51]. In Germany power lines are planed to distribute offshore generated energy to the inland [11, 12, 51], but ongoing protests hamper these developments and have led to changes in the plans [1, 28]. Physical problems of long-distance transmission are an increased grid load and vulnerability to large scale blackouts due to cascading failures [44, 49, 55].

Renewable power sources typically are connected to the grid via inverter-based generators, while conventional power plants operate with synchronous machines [48]. Synchronous machines have inertia to maintain the frequency at a fixed value. Inverters transform the DC power from, e.g. wind power generators, into an AC power with a frequency suitable for the grid. Theses two types of generators have different characteristics and dynamics [24, 66]. Most current control mechanisms depend on the inertia of synchronous machines. An increased share of inverter-based generators demands other approaches to regulate frequency deviations for preventing blackouts [24].

The dependence of wind and solar power on the weather conditions causes a high variability of these power sources [62] . The statistic properties of these fluctuations determine the dimensioning of storage technologies and the optimal composition of available renewable energy sources [19, 62].

3.4.1 Variability of Wind Power Generation

Reliability of power supply is of central importance, since other infrastructures and sectors are highly dependent on it. It is crucial to provide enough power, but the grid load must not increase too much, to prevent blackouts [2, 24, 49]. Because wind power and solar photovoltaic are highly dependent on weather conditions, they are intermittent and cannot be flexible switched on when needed [48, 65]. It is important to understand their variability to enable a steady power supply at all times [62]. Adequate forecasts help to appropriately dimension backup technologies, to compensate fluctuations in power generation [19] and to avoid large deviations of power grid frequency [24] and therefore blackouts.

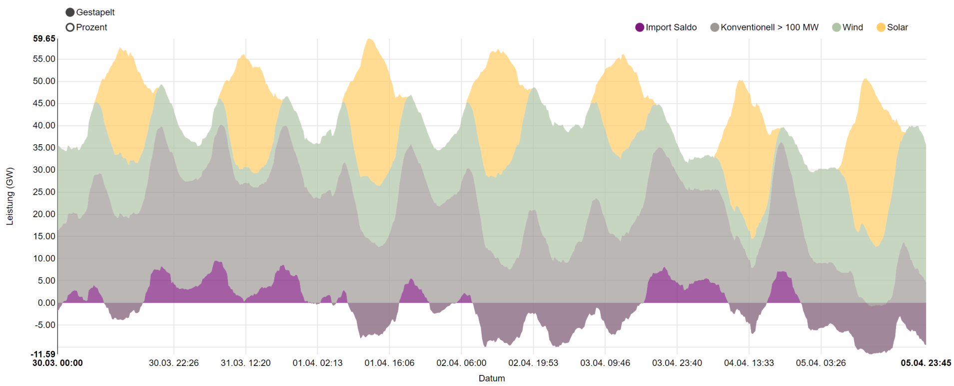

Figure 3.3: This plot shows the share of conventional and renewable energy sources together with the imported energy for the 14th week of 2020 in Germany. It impressively shows the possible variations of renewable energy sources. At the 4th of April around 8 p.m. there is hardly any renewable energy generated. About 16 hours later, the next day around 12 noon, renewable energy provides 50GW, which equals the demand, leading to a surplus production of conventional power, meaning that power from conventional sources needs to be exported to ensure grid stability.
(Source: Fraunhofer ISE, graphics/diagrams: B.Burger, *Electricity production in Germany in week 14 2020*. https://www.energy-charts.de/power_de.htm?source=conventional&year=2020&week=14, visited: 08.07.2020.)

Especially the time series of wind power generation needs to be well understood [62], since solar photovoltaic mostly follows daily and seasonal cycles with yearly recurring patterns, whereas wind power shows more irregular variations [50]. Furthermore, German dependence on wind power is intended to increase strongly [19, 50].

Wind variability can be observed on time scales from seconds over minutes [2], to seasonal [13, 26], interanual [13], decadal and multidecadal variability [67]. This variability leads to fluctuations and related low and high wind power generation phases, which last from seconds to weeks [62].

The requirements for backup and storage technologies will be crucially determined by extreme events of either low or high power generation and their duration [19, 50, 62]. Winter months are particularly relevant, as solar power generation is rather low and the German peak load occurs in winter [26, 50]. Short events of low power generation are frequent, very long events are much rarer [50]. They are generally most frequent in summer and least frequent in winter. Autumn and spring are mostly close to the yearly average. Nevertheless the maximum duration is more evenly distributed between the months and relevant low wind events occur throughout the year [50].

The study of data for 40 years (1980 to 2019) by Ohlendorf et al. [50] comes to the conclusion that in Germany a period of around five consecutive days, during which the average wind power generation is below 10% of the installed capacity, is to be expected every year. Every tenth year nearly eight consecutive days are to be expected. When only considering winter months the duration reduces to less than three days or less than five days every tenth winter respectively. Ohlendorf et al. [50] further recommend to consider multiple weather years when modeling phases of low wind power generation. If only one year is considered it is likely to significantly underestimate the occurrence and persistence of extreme wind power events and their implications for the energy system [13, 50, 67].

3.4.1.1 Persistence in Wind Power Generation

The persistence statistic of wind power generation is an important influencing factor for future renewable energy systems with a high share of wind power, as intended for Germany. Weber et al. [62] investigated the persistence statistic of wind velocities and wind power generation, meaning the duration of periods with wind velocities (wind power generation) constantly below or above a certain threshold.

To forecast the occurrence of extreme wind events the tails of the distribution are of special interest. If the events of crossing the threshold follow a Poisson process, as intuitively expected, the persistence statistic would follow an exponential distribution with a kurtosis of 9 (cf. sec. 2.2.2.2). Larger values for the kurtosis indicate heavy tails (cf. sec. 2.1.4.4). The investigations of Weber et al. [62] show a kurtosis much larger than 9, for both low and high wind velocity events, for several locations in Europe. Therefore, the waiting time distribution is not well approximated by exponential distributions. Instead q-exponentials give a better fit as shown in figure 4 of the paper [62].

Not only wind velocities but also wind power generation shows a high persistence of low and high wind power generation periods. Especially periods of low-wind power generation show higher persistences as expected based on a simple Poisson process.

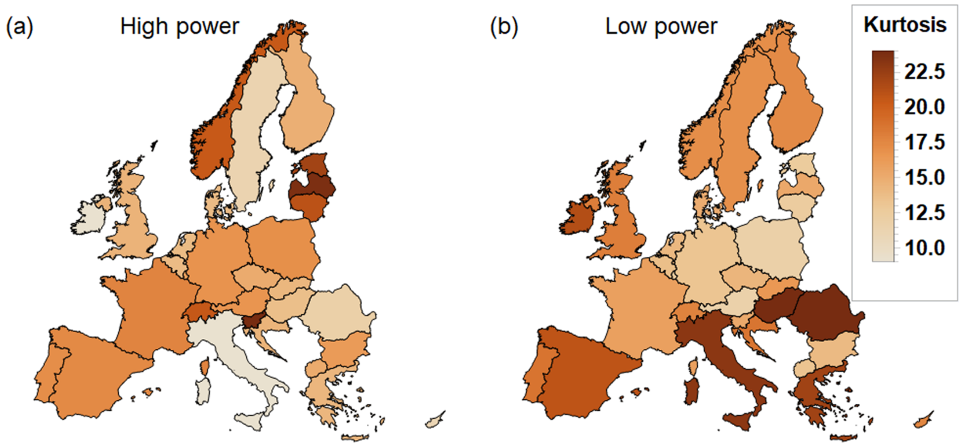

Figure 3.4: The persistence statistics of wind power generation in Europe are heavy tailed.
(Source: Weber et al. [62] *Wind Power Persistence Characterized by Superstatistics*, fig. 6.)

Particularly the persistence of periods of low and high wind power generation are important to dimension backup and storage technologies for future energy systems [62]. The calculated q-exponential distributions could be helpful for that [62].

3.4.2 Backup and Storage Technologies

Variability of renewable power sources poses a major challenge for highly renewable energy systems which mostly rely on wind and solar power. Therefore well-matched backup and storage technologies are needed additionally to provide energy in accordance with the demand [19, 24]. Pumped hydro storage, adiabatic compressed air reservoirs, batteries, interruptible loads (demand-side-management), geothermal energy, biomass energy, power-to-gas and power-to-heat are the mainly considered technologies to compensate fluctuations [19, 58].

During periods of low renewable power generation, the demand must be satisfied by backup power plants and electricity storage. Interruptible loads can be switched off. If the energy generation is higher than the demand, storages can be filled, to provide energy for the next shortage. Furthermore interruptible loads can be switched on to optimally use the surplus power [19]. Hence a well balanced composition of fluctuating renewable energy sources with backup and storage systems is key to a reliable sustainable power system.

Fluctuations on different scales require different needs for backup technologies. Extreme situations and their persistence crucially determine which compensating technologies are needed, as well as their scale [19, 62]. Ohlendorf et al. [50] suggest investigating both hours with the power generation constantly below a threshold and hours with the mean below a threshold. Time series of these two kinds of shortages show different patterns, which result in different needs for compensating technologies. Therefore a better statistical understanding of the fluctuations and extreme conditions allows an improved design of future electricity grids. A full analysis of scales on which each compensating technology could operate, as well as possible compositions of renewable energy sources with backup technologies, is given in *Flexibilitätskonzepte für die Stromversorgung 2050* [19].

3.5 Wholesale Electricity Prices in Germany

The market price $p(t)$ for electricity at a time t is determined such that supply and demand are balanced

$$S(p(t), t) = D(p(t), t). \tag{3.1}$$

The demand for electricity is strongly inelastic [46], i.e. it depends only weakly on the prices. Therefore, this dependency will be neglected in the following. To understand the evolution of market prices, we must thus analyze

- how the supply S generally depends on the price p,
- how the supply curve $S(p)$ changes in time due to the availability of renewable power and
- how the demand D depends on time due to human and economic activities.

Typically, power plant operators will only offer electricity if the wholesale electricity price exceeds the variable costs of power generation, since otherwise marketing would lead to losses. As a consequence, power plants with low variable costs run most of the time to satisfy the base demand, while power plants with high variable costs typically only run during periods of high demand. The costs differ strongly between the types of power plants. A ranking of power plants according to the variable costs – from low to high – is commonly referred to as the merit order curve. When looking at conventional power, nuclear and brown coal power plants typically have high fixed, but low variable costs. In contrast, gas and oil fired power plants typically have much higher variables costs. Electricity from wind and solar power plants have neglectable variable costs and therefore have the highest priority according to merit order curve. When looking at the merit order curve, it can therefore be seen that the wholesale price usually increases monotonic with the demand (cf. fig. 4.1d and fig. 3.5).

During periods of high renewable power generation, the supply curve $S(p, t)$ is shifted to the right, meaning that providing energy from sources with high variables costs becomes less profitable and therefore less likely. If the demand remains constant, this leads to lower wholesale electricity prices $p(t)$. Therefore, the variability of renewable power sources is crucial for the development of electricity prices.

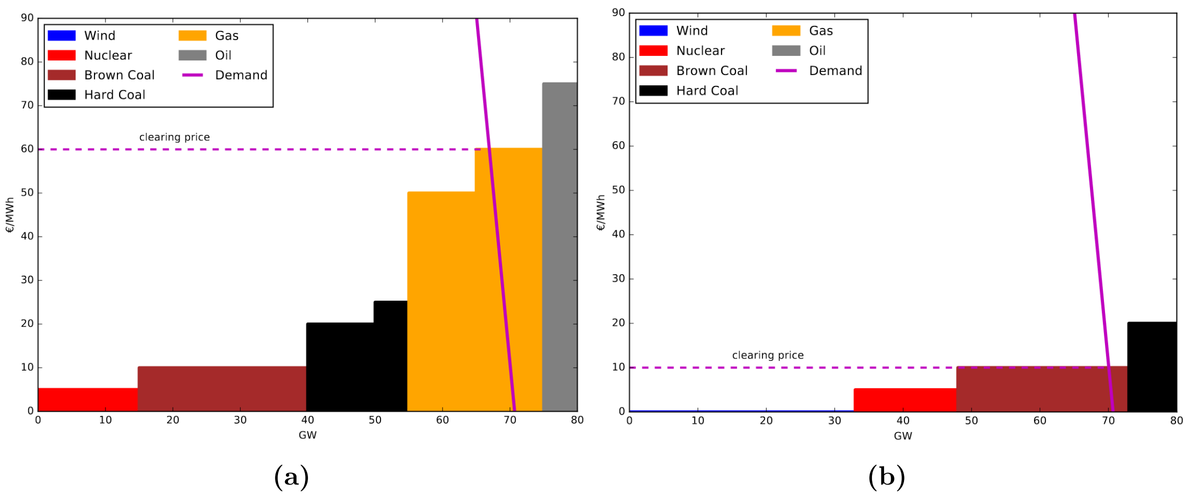

Figure 3.5: Renewable power generation influences the electricity prices and the merit order curve. **(a)** With no power from variable renewable power sources it is profitable to provide power from power plants with high variable costs, like gas fired power plant. **(b)** If renewable power can be provided and the demand remains constant, the merit order curve dramatically shifts to the right. The market clearing price lowers and it is not profitable to provide power from power plants with high variable costs.

(Source: Tom Brown, *Energy System Modelling* [10], lecture 7, slides 9 and 10.)

As the share of variable renewable energy increases, so does their influence on the wholesale electricity prices. To capture the impact of variable renewable power generation on the emergence of electricity prices, it is useful to introduce the residual load. This quantity is defined as the difference of the total grid load and power generation from the variable renewable power sources, wind and solar:

$$RL(t) = L(t) - W(t) - P(t). \tag{3.2}$$

Since storage technologies for electrical power are limited, the residual load must be satisfied by dispatchable power plants, meaning power plants that can be flexibly used, such that the demand matches the supply to ensure grid stability [19, 24]. The residual load varies strongly in time, because in addition to the variability of wind and solar power (cf. sec. 3.4.1), the demand for electricity strongly changes within a day. Typically, it peaks in the morning and the evening and is significantly lower during the night, with demand patterns changing between workday and weekend and between seasons (cf. fig. A.6) [25].

The simplified treatment above does not consider changes in the availability and the variable costs of dispatchable power plants. However, in reality notable exceptions do exist. After the Fukushima Daiichi nuclear disaster, more than 11GW of nuclear generation capacity were temporarily unavailable in Germany [25]. In the absence of such exceptional events, we can assume that changes of the the merit order curve of dispatchable power plants are mostly limited to long time scales. This can be understood as market prices of fossil fuels can change rapidly, but plant operators typically have long-term supply contracts and power plants are in operation for decades. Since this thesis focuses on the intra-annual variability of electricity prices, the merit order curve of the dispatchable power plants will be approximated as constant.

Furthermore, one can regularly observe negative electricity prices at the EPEX SPOT market – a surprising effect which is not explained by the reasoning above. This phenomenon is rooted in the low flexibility of nuclear and brown coal power plants. They cannot freely adjust their generation to the current residual load. If the residual load is very small, these power plants should in principle reduce their generation, but this can be costly or even impossible due to technical restrictions. Hence, it can be beneficial for plant operators to deliver power at negative prices, meaning they have to pay to provide energy. To deal with the flexibility issue, some market models treat nuclear and brown coal power plants different than dispatchable power plants [25]. Early studies of negative electricity prices, stressing the importance of wind power generation and the lack of flexibility, can be found in [22, 60].

The considerations of this section provide a useful starting point to understand the dynamics of electricity prices. They lay a foundation for the examination in chapter 4. However, it is obviously only an approximation and misses interesting non-linear and non-statistical effects.

3.5.1 Electricity Market

Electricity is mostly traded in advance of the time when it is actually consumed. Day-ahead trading in Germany is implemented by the European Power Exchange EPEX SPOT, a part of the European Energy Exchange (EEX) [20]. Intra-day trading is also offered for Germany, but with a smaller trading volume. For the entire region covered by EPEX SPOT the day-ahead trading volume has been around 468TWh, compared to 62TWh for intra-day trading in 2016 [20]. Therefore, the prices evaluated for this thesis are day-ahead prices.

4 Persistence in Electricity Prices

Renewable power generation strongly influences the electricity market price. Recalling the considerations in section 3.5, a strong anti-correlation between price and renewable energy generation is expected. When wind and solar power generation are high, wholesale electricity prices should be low and vice versa. As a consequence the electricity price time series might show similar statistical features as the renewable power generation time series. Inspired by the heavy-tailed persistence statistic of wind power generation (cf. sec. 3.4.1), I will focus on the persistence statistics of electricity prices, i.e. the duration of periods where the wholesale electricity price is below or above a certain threshold. Is the distribution of these periods heavy-tailed? Do exceptional long period of constant low or high prices exist?

To answer these questions, I will start by looking at different influencing factors on the wholesale electricity price and examine whether the price really decreases with a higher share of renewable energy. Price time series show strong recurring patterns on the time scale of days, weeks and seasons. The statistical analysis therefore requires a normalization of the price time series. I will introduce different methods and calculate the persistence of these normalized price time series to see if they show the same persistence statistic as wind power generation does. These investigations will be done for the German electricity market for the year 2016 and could be repeated for more years in order of further research.

4.1 Influencing factors

As a first step the statistical factors influencing the electricity prices need to be identified. Figure 4.1 shows a histogram of the wholesale electricity prices and different external factors. Wind and solar power generations, as well as load and residual load are considered. The correlation between price and the respective possible influencing factor is calculated with the different methods, detailed in section 2.3.2.

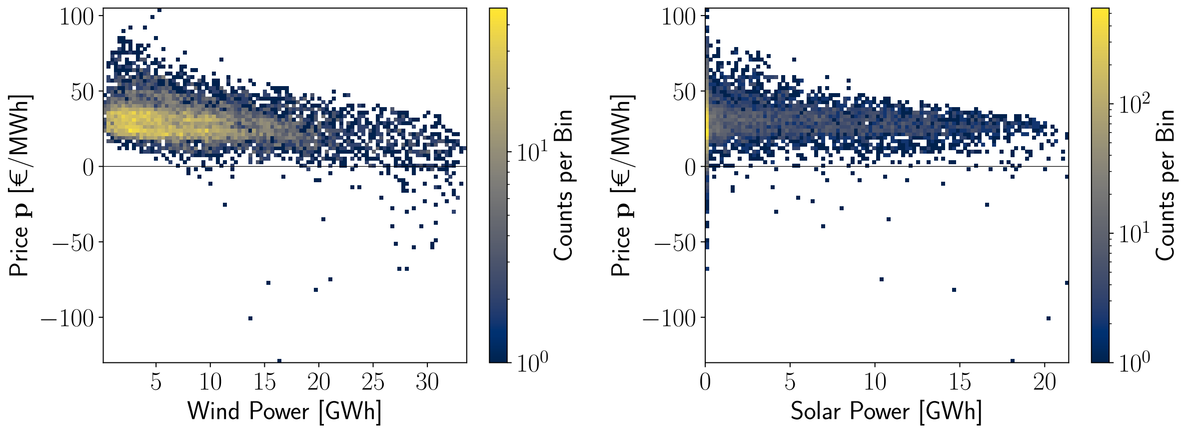

(a) $\tau = -0.2306$, $\rho = -0.3382$, $r = -0.4033$

(b) $\tau = 0.0323$, $\rho = 0.0502$, $r = -0.0957$

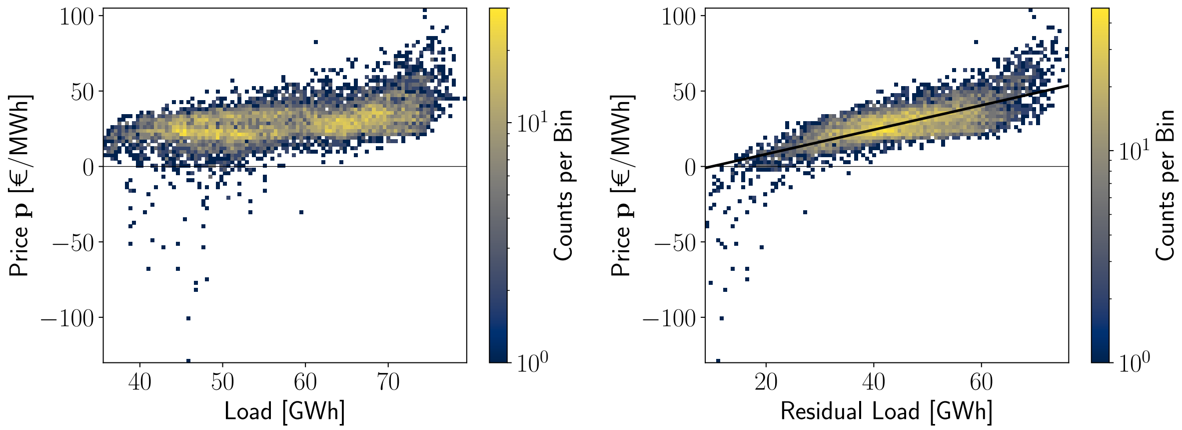

(c) $\tau = 0.3547$, $\rho = 0.5168$, $r = 0.5067$

(d) $\tau = 0.5197$, $\rho = 0.7018$, $r = 0.7377$
Linear fit: $p(\text{RL}) = a \cdot \text{RL} + b$ with residual load RL and parameters $a = 0.80935 \pm 4 \cdot 10^{-5}$, $b = -8.025 \pm 2 \cdot 10^{-3}$.

Figure 4.1: The wholesale electricity prices for Germany of 2016 are plotted against the four possible influencing factors wind, solar, load and residual load. Each data point represents one hour. The correlation coefficients Kendalls's τ, Spearman's ρ and Pearson's r are calculated (cf. sec. 2.3.2).

Wind power generation and wholesale electricity price are anti-correlated as expected from the previous discussion. The correlation coefficients lie between -0.2306 and -0.4033 and the variance of the price is still rather large (cf. fig. 4.1a).

In contrast, solar power generation and electricity prices are only weakly correlated (cf. fig. 4.1b). This might originate from the fact that solar power generation is especially high at times where the load is also high (cf. fig. A.4c and fig. A.6c). Since generally the price increases with a higher load this opposing effect might overlay the price reduction due to renewable power generation and therefore lead to a vanishing correlation, even though the statistical dependence between solar power generation and the decrease of electricity prices might still be given. Furthermore, the installed solar capacity is lower than for wind and periods of high solar power generation are rather infrequent. As a consequence the detection of a statistical dependence could be impeded.

Concluding from these findings electricity prices indeed decrease with a higher share of renewable energy, but a negative correlation can only be seen for wind, not for solar power generation. The mixture of both variable renewable energy sources also shows a negative correlation with the wholesale electricity price, but it is not as strong as it is if only wind is considered (cf. fig. 4.1a and fig. A.2).

Load and wholesale electricity prices are positively correlated as expected. Typically, an increase of the demand leads to an increase of the electricity price. The strength of the correlation is moderate, but clearly stronger than for wind power generation (cf. fig. 4.1c).

The impact of the load and the renewable power generation can be combined using the residual load introduced in section 3.5. Residual load and wholesale electricity prices are strongly correlated, with both Pearson's r and Spearman's ρ exceeding 0.7. The increase of the price with the residual load is clearly visible in figure 4.1d. To further quantify this dependence, I include a linear regression (cf. sec. 2.3.2.1)

$$p(\mathrm{RL}) = a \cdot \mathrm{RL} + b, \tag{4.1}$$

which yields the parameters $a = 0.80935 \pm 4 \cdot 10^{-5}$ and $b = -8.025 \pm 2 \cdot 10^{-3}$. This fit captures the dependence of the price p and the residual load RL for the given data set. Notable outliers exist for very low and very high values of the residual load, where much more extreme values of the price are observed.

4.2 Normalization Methods

The residual load shows strong recurring patterns on the time scale of days, weeks and seasons (cf. fig. A.7). The residual load peaks in the morning and the evening and is significantly higher in winter than in summer. Due to the high correlation these recurring patterns are also present in the electricity price time series and complicate a statistical analysis. To circumvent this problem it is therefore important to clear the electricity prices by the effects of the load, since otherwise the persistence would not be longer than the magnitude of one day for most of the thresholds, due to daily patterns (cf. fig. A.8c).

The basic idea of time series normalization is to consider the difference or the quotient of the raw electricity prices and a reference time series, which captures the recurring patterns of the price. Three different reference time series are used and compared in this thesis.

The first method is directly based on the evolution of the residual load. As a reference time series we use the linear regression (cf. eq. (4.1)) with the actual residual load of the respective time interval. It must be noted that this approach can capture recurring patterns in the price only if they arise similarly in the time series of the residual load and the linear fit does not well capture extremely low or high prices (cf. fig. 4.1d).

As a more direct option the average weekly price profile is used as a reference time series. For each hour of the week, the price is averaged over all weeks of the year leading to the profile shown in figure 4.2a. For this method the standard deviation is rather high, showing potential limitations of this approach. The high standard deviation is partly due to the negligence of seasonal patterns (cf. fig. A.8).

To reduce the influence of seasonal changing patterns, separate standard profiles for every quarter are calculated. Since the weekdays show comparable patterns they are combined for one average. Saturdays and Sundays show different patterns, which is why they will be evaluated separately.

In general, the quarterly standardization shown in figure 4.2b-e shows a lower standard deviation than normalizing the week with an annual average (cf. fig. 4.2a). Especially in the second and third quarter the standard deviation is generally low. When looking at the Sundays of the second quarter they show a very high standard deviation. Since for the days on the weekends only about 12 data points are taken for every quarter, even one exceptional event could dramatically increase the standard deviation.

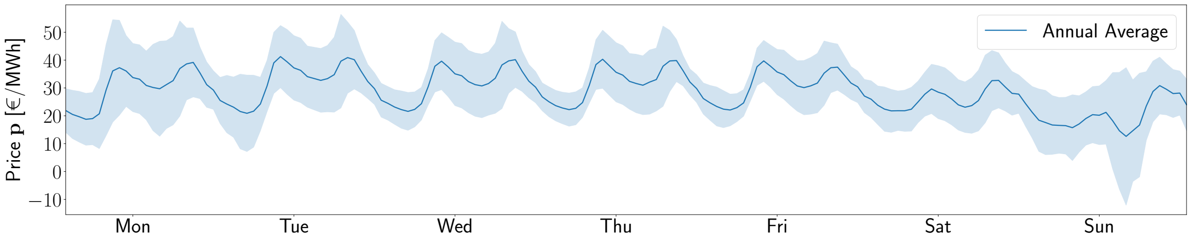

(a)

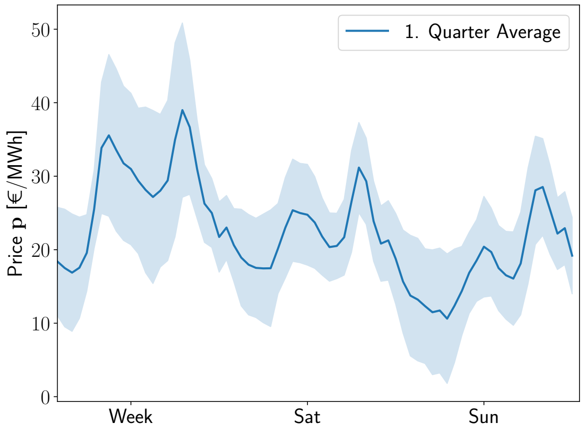

(b)

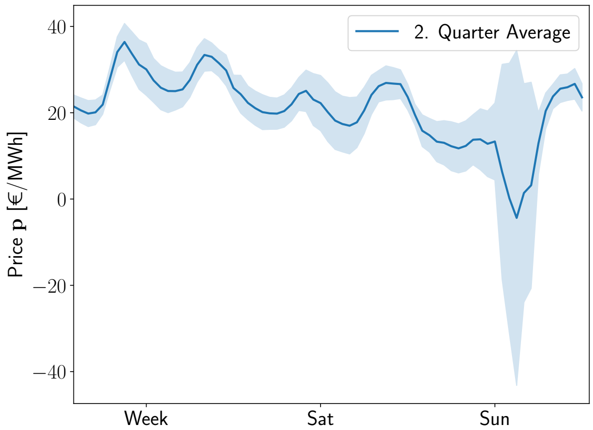

(c)

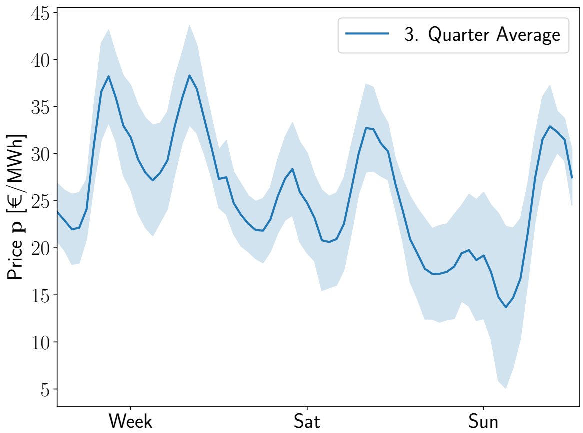

(d)

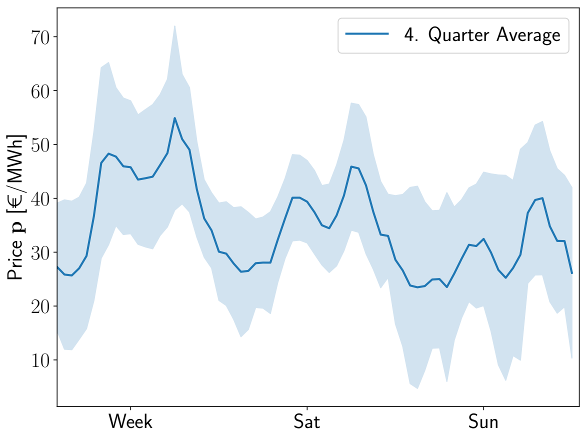

(e)

Figure 4.2: Reference time series for normalization. **(a)** The average electricity price trajectory for one week averaged over the whole year is plotted together with the standard deviation (shaded area). Equivalent to the trajectory of the load (cf. fig. A.6) a difference between weekdays and weekends is clear to see. **(b-e)** The average price for weekday, Saturday and Sunday is plotted separately for every quarter together with the standard deviation. The general trends are the same for all quarters, but the average price and the magnitude of the standard deviation varies between the quarters.

This three reference time series are now used in two different ways to compute a normalized electricity price time series. Either the reference time series is subtracted from the actual price or the actual price is divided by the reference time series. In total this leads to six different normalization methods for the price time series (cf. fig. 4.3).

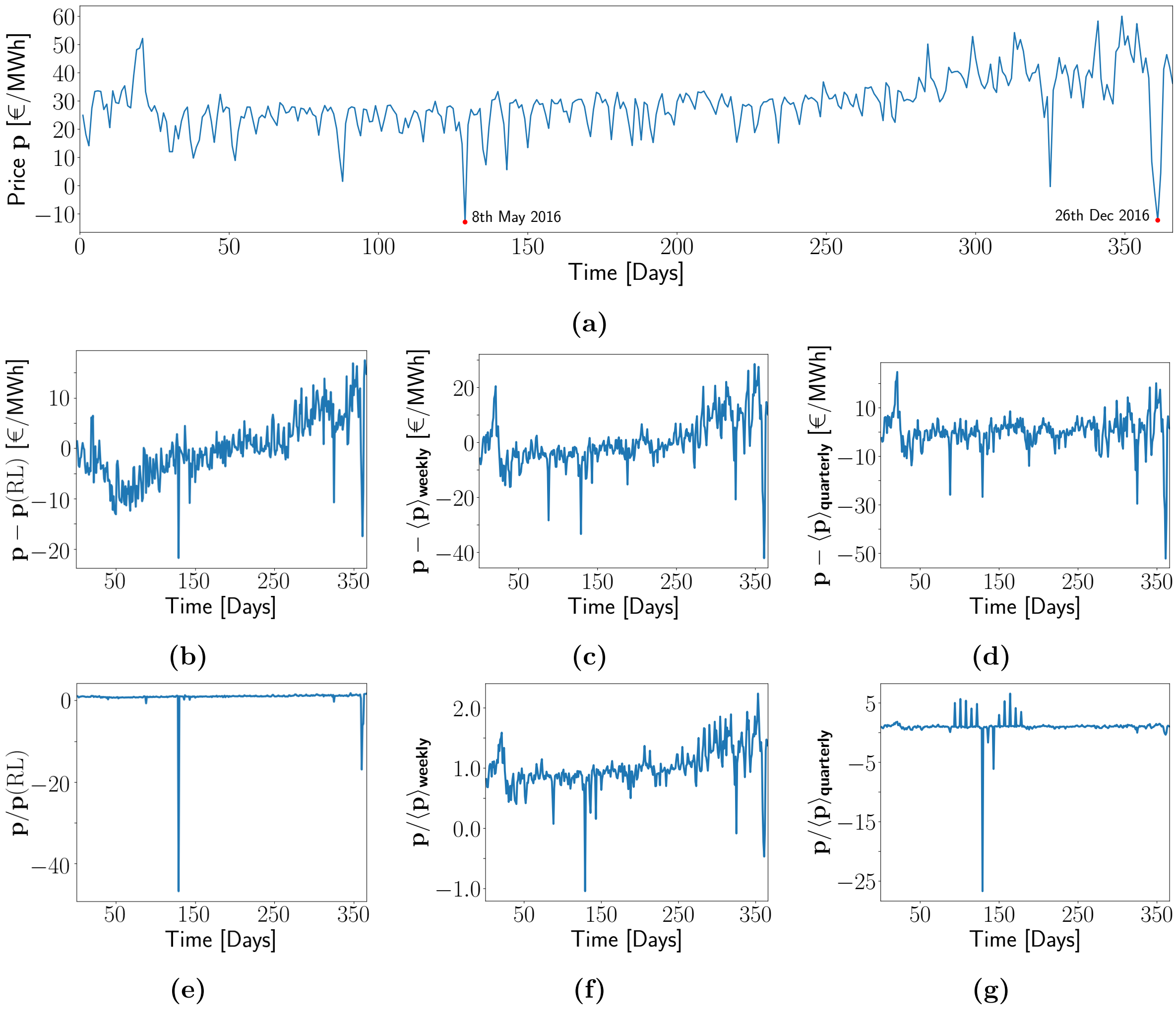

Figure 4.3: Wholesale electricity price time series in Germany for 2016 plotted as the daily mean. **(a)** Day-ahead prices from the EPEX SPOT market. Huge price deviations can be observed including occasional negative electricity prices (cf. sec. 3.5). **(b-g)** For further analysis, the price time series is normalized to absorb the effect of recurring pattern and the electricity demand. **(b,e)** Normalization using the function $p(\mathrm{RL})$ obtained from the linear fit in figure 4.1d. **(c,f)** Normalization using the weekly price pattern $\langle p\rangle_{weekly}$ shown in figure 4.2a. **(d,g)** Normalization using separate patterns for every quarter year $\langle p\rangle_{quartely}$ as shown in figure 4.2b-e.

Figure 4.3 compares the normalized time series to the original electricity price time series. All methods show variations in the daily mean price. In the original day-ahead price time series, weekly patterns are clearly visible (cf. fig. 4.3a). As desired these recurring patterns are largely absent in the normalized time series.

Furthermore, the original day-ahead price time series shows a strong seasonal pattern. Typically, prices are higher and more variable in winter than in the summer. These seasonal patterns remain present by normalizing with the weekly pattern $\langle p \rangle_{weekly}$ and the linear fit $p(\mathrm{RL})$ using the residual load time series (cf. eq. (4.1)). In fact, the seasonal effects are the strongest for the time series $p - p(\mathrm{RL})$.

We conclude that the reference time series $\langle p \rangle_{\mathrm{quarterly}}$, which resolves the four quarters of the year, is needed to remove the seasonal patterns in the normalized time series. However, in the second quarter huge variability can be observed for the normalized time series $p/\langle p \rangle_{\mathrm{quarterly}}$ (cf. fig. 4.2c). The exceptionally high and low peaks correspond to the 13 Sundays of this quarter where the denominator $\langle p \rangle_{\mathrm{quarterly}}$ is very low (cf. the discussion in [18]).

Negative electricity prices (cf. sec. 3.5) occur in all methods. There are two days with a high negative daily mean price which can be seen in every time series, but especially good in figure 4.3e. On the 8th of May 2016 Mother's Day, a public holiday, causes a low demand, but the weather was sunny and windy, leading to surplus power supply [57]. On the 25th of December 2016 the mild winter and public holidays causes a low demand but wind causes high power generation. This leads to a surplus power generation and therefore negative electricity prices [27].

4.3 Persistence Statistics

For a good statistical analysis it is important to eliminate daily, weekly and seasonal patterns due to the influence of the load. As discussed in section 4.2 the reference time series $\langle p \rangle_{\mathrm{quarterly}}$, which resolves the four quarters of the year, is best suitable to remove the recurring patterns in the time series. This is why I will only take a closer look at $p/\langle p \rangle_{\mathrm{quarterly}}$. Results for the other methods are summarized in the appendix.

Equipped with this normalization method I analyze the waiting time distribution (cf. sec. 2.2.2) for different thresholds. As there are periods of high wind power generation as well as periods of low wind power generation, this calculation is done for the price being below and above a threshold. In particular, I evaluate the duration τ of all periods in which the normalized price time series is constantly lower or higher than a given threshold.

Appropriate values for the threshold are obtained from the 10%, 25% and 50%-quantil (periods below threshold) and the 50%, 75% and 90%-quantil (periods above threshold). In figure 4.4 histograms of the waiting times are plotted together with an exponential maximum-likelihood fit, $\exp(-\lambda_e \cdot \tau)$, where $\lambda_e = 1/\text{mean}$ (cf. sec. 2.3.1.1), to see how well the waiting time distribution can be approximated by an exponential distribution. The sample kurtosis κ is calculated, to compare it to the kurtosis $\kappa = 9$ of an exponential distribution.

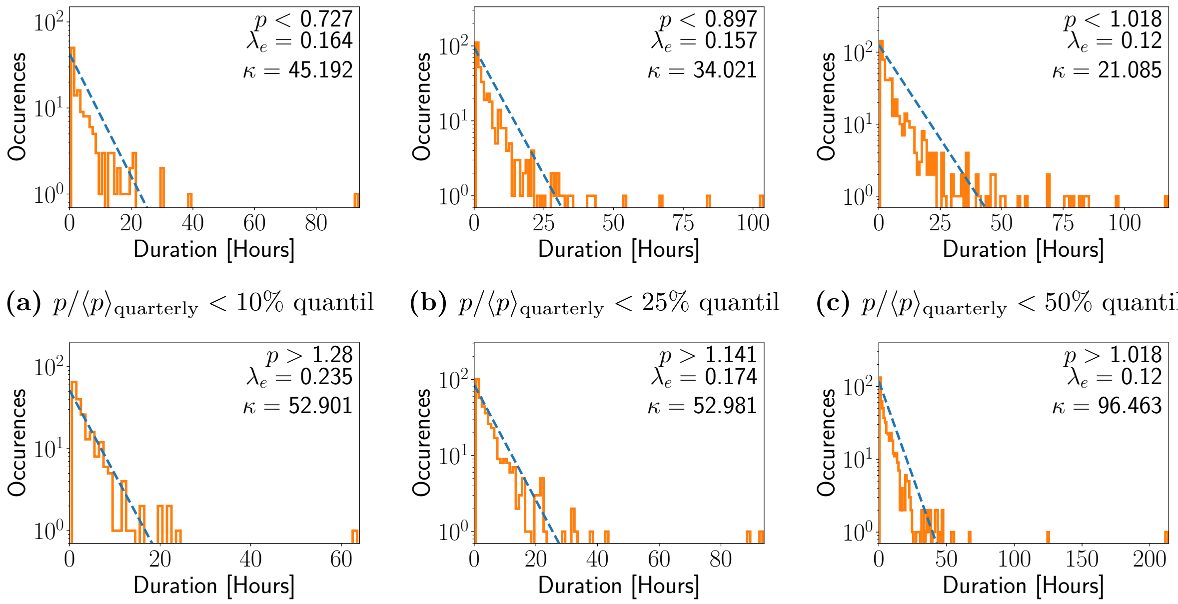

(a) $p/\langle p \rangle_{\text{quarterly}} < 10\%$ quantil **(b)** $p/\langle p \rangle_{\text{quarterly}} < 25\%$ quantil **(c)** $p/\langle p \rangle_{\text{quarterly}} < 50\%$ quantil

(d) $p/\langle p \rangle_{\text{quarterly}} > 90\%$ quantil **(e)** $p/\langle p \rangle_{\text{quarterly}} > 75\%$ quantil **(f)** $p/\langle p \rangle_{\text{quarterly}} > 50\%$

Figure 4.4: Persistence of the electricity price time series for Germany in 2016 normalized as $p/\langle p \rangle_{\text{quarterly}}$. Orange bars give the histogram of the duration of periods where the normalized price time series $p/\langle p \rangle_{quartely}$ is **(a-c)** below a given threshold and **(d-e)** above a given theshold. The blue dashed line shows an exponential maximum-likelihood fit with exponent λ_e. The kurtosis κ for the data is calculated as described in equation (2.11).

The duration of periods with very high or very low prices, i.e. above the 90% quantil or below the 10% quantil, appears to be well described by the exponential fit (cf. fig. 4.4a and 4.4d). However, in both cases there is a single period of extraordinary duration (longer than 60 and 80 hours, respectively), which leads to a large value of the sample kurtosis. A similar behavior is found when modifying the threshold value. The exponential fit describes the bulk of the data reasonably well, but several outliers exist. Choosing the 50% quantil as the threshold, a significant asymmetry between periods above and below threshold can be observed. Outliers are rare but extreme for the period above 50% quantil, leading to an extremely high value of the sample kurtosis.

The maximum duration of the waiting time depends on the threshold and lies between 2.5 and 9 days, which is the same magnitude as the duration of high or low wind power generation periods [50, 62]. Surprisingly all, except one, events of maximum duration lie in December. Four days of normalized electricity prices above the 75% quantil (14th of Dec. - 18th of Dec.) are shortly after followed by five days of the normalized electricity prices below the 25% quantil (22nd Dec. - 27th Dec.). When looking at the waiting times of the price below or above the 50% quantil the opposing phases almost directly merge into one another. This behavior could be explained with general low solar power generation, combined with a high but strongly fluctuating demand, in combination with long periods of high and low wind power generation. In fact, in December of 2016 some parts of Germany were colder, other parts of Germany were warmer than expected [64] and at the end of the year wind power generation was exceptionally high [27].

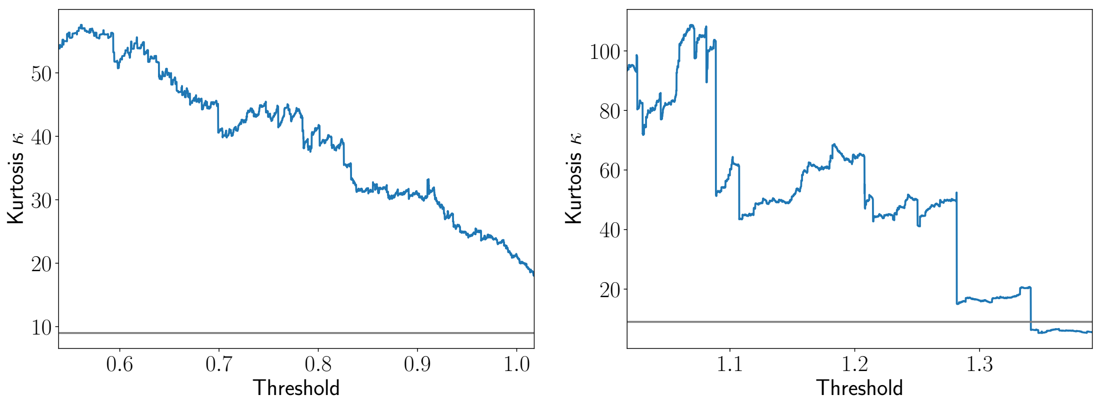

(a) $p/\langle p \rangle_{\text{quarterly}}$ below threshold **(b)** $p/\langle p \rangle_{\text{quarterly}}$ above threshold

Figure 4.5: Kurtosis of the waiting time distribution as a function of the threshold value. The plots shows the sample kurtosis for the duration of periods where the normalized electricity price is constantly **(a)** below and **(b)** above the threshold. The range of threshold values in the plots correspond to **(a)** the 5% - 50% quantil and **(b)** the 50% - 95 % quantil. The solid black lines show the kurtosis value for an exponential distribution $\kappa = 9$ for comparison.
The whole range of thresholds can be seen in figure A.15 and figure A.16.

To further quantify the likeliness of long periods, the kurtosis is plotted as a function of the threshold value (cf. fig. 4.5). For the price being below the threshold the range between the 5% and the 50% quantil is investigated more closely. For the price being above the threshold the range between the 50% and the 95% quantil is investigated more closely.

Electricity prices show persistence of low and high price states with a kurtosis higher than $\kappa = 9$ for most of the thresholds within a range of 45% of the data points (cf. fig.4.5). The time series of the normalized electricity prices displays more outliers than expected based on a simple exponential distribution. Heavy tails in the waiting time distribution can be observed.

The kurtosis for the normalized price $p/\langle p\rangle_{\text{quarterly}}$ below a threshold is the highest for thresholds near the 5% quantil and decreases nearly monotonically decreases as the threshold gets higher (cf. fig. 4.5a). The kurtosis for the normalized price $p/\langle p\rangle_{\text{quarterly}}$ above a threshold is the highest for thresholds near the 50% quantil and nearly monotonically decreases with higher thresholds (cf. fig. 4.5b). The jumps of the kurtosis values in figure 4.5b might originate from the fact, that the normalized price time series $p/\langle p\rangle_{\text{quarterly}}$ is very flat and smooth. Slight changed in the threshold can have a huge impact. Therefore, a tiny increase of the threshold might lead to the disappearance of some of the very long events.

Surprisingly, the behavior of the kurtosis is opposite for low and high electricity prices. I expected the kurtoses to decrease the closer the threshold gets to the marginal quantils, which is indeed observed for firgue 4.5b. In this manner the two figures 4.5a and 4.5b would look similar but mirrored. Accordingly the graph in figure 4.5a should be the other way around, so that the kurtosis increases with thresholds closer to the 50% quantil. However, the opposite behavior is shown in figure 4.5a. The reason for the true trajectory can be found when taking a closer look at the location of the quantil boundaries. The 5%, 50% and 95% quantil boundaries are very close together compared to the whole range of possible values, since the narrow distribution of values in the normalized price time series leads to a very sharp peak in the kurtosis plots (cf. fig. A.15f and A.16f). The quantil boundaries even lie within this narrow value range of the peak. Therefore, a detailed look at such small value domains is sensitive to statistical and non-statistical market influences and small changes in the threshold lead to heavy changes in the kurtosis. Nevertheless, the results shown in the figure 4.5 are feasible to describe the general trend in the waiting time distribution of the electricity price time series.

It is reasonable to conclude, from the results shown in figure 4.5, that the waiting time distribution of the electricity prices is heavy tailed and therefore not well described by an exponential distribution. To reach a final conclusion, a longer data set would be needed enabling further statistical tests.

The observed persistence does not necessarily have to originate from periods of high wind power generation, but it is very likely that wind power generation has a measurable impact on the market pricing of electricity and the persistence statistics.

Wind power generation investigated by Weber et al. [62] showed persistence values up to about $\kappa = 25$. The kurtosis calculated for the electricity prices is much higher for the vast majority of the thresholds. The kurtosis values might seem too large, but the maximum duration of high and low electricity prices has the same magnitude as the duration of low or high wind power generation periods. Moreover, seasonal and non-statistical market effects strongly influence the market pricing and the normalization will not always be suitable to erase all market and load effects.

The calculations could be enhanced by treating public holidays during weekdays as Sundays because they show equal price patterns. However, considering the large uncertainties of the methods this might only have a minor effect on the calculations.

More important influences on the calculations might arise from small data sets. Especially for the method of calculating averages for every quarter, the data set might be too small for calculating a reliable pattern. The other methods have a larger data basis, but seasonal effects are clearly visible, which strongly influences the calculations. Furthermore, as presented in section 2.3.1.2 the kurtosis can get misestimated for small data sets. The waiting time distributions have rather few data points, which might hamper the calculations. However, in general small data sets lead to smaller kurtoses, which is why this effect should not influence the trends seen in the investigations. Nevertheless, one exceptionally long event will strongly influence the calculations.

Looking at the price time series normalized by $p/\langle p\rangle_{\text{quarterly}}$ (cf. fig. 4.3g) the time series is very smooth, disregarding a few exceptions. This leads to the threshold being very close to the data points most of the time. Taking into account uncertainties these investigations can only give an orientation for further research.

Overall the investigations show a negative correlation between wind power generation and the wholesale electricity price. Strong persistence in electricity prices can be observed similar to the findings of wind power generation by Weber et al. [62]. Further research would have to clarify the findings by examining data for several years.

5 Conclusion

Wind and solar power are essential for the decarbonization of our energy supply, but their intrinsic variability challenges system operation. At the same time, renewable power generation strongly influences the pricing of electricity. Therefore, electricity price and renewable power generation might share essential statistical features. In this thesis, I investigated the persistence statistics of the wholesale electricity price time series for the German market in 2016. I examined the influence of different factors on the price formation and analyzed the persistence of low/high price states in comparison to the exponential waiting time distribution of simple stochastic processes.

Wind power generation shows negative correlation with the electricity prices and in periods of high wind power generation occasional negative electricity prices can be observed. Solar power generation also seems to lower the wholesale electricity prices, even though the calculated correlation vanishes. Days with a high solar power generation also occasionally show negative electricity prices. This leads to the conclusion that a higher share of renewable energy indeed lowers the wholesale electricity price, which is the first central finding of this thesis.

The analysis of the waiting time distribution for the electricity prices being below or above a certain threshold shows that the majority of the data could be approximated by an exponential distribution. However, outliers exist with a duration of several days, up to ten times as long as the mean. The existence of outliers strongly increased the sample kurtosis κ compared to the value $\kappa = 9$ of an exponential distribution. These results indicate that the wholesale electricity prices have a heavy tailed waiting time distribution although non-statistical effects influence the electricity prices. Furthermore, I tested different normalization methods to remove recurring patters, but they cannot fully compensate the effects of the load on the electricity prices.

The calculations in this thesis have exemplary been done for 2016. For further research the calculations could be repeated for additional years, to generate a broader data basis.

As stated in section 3.4.1 effects can be misjudged if only looking at one year. Nevertheless one has to be careful when investigating long time spans. Non-statistical market effects, different shares of renewable energy and laws like the "EEG-Umlage" influence the wholesale pricing of electricity. Furthermore the change in variable costs of conventional power plants has a greater impact when looking at larger time scales. Beyond that, wind power generation varies between years, which might lead to a changing influence on the price.

For this work the correlation between the day-ahead prices and the actual power generation has been investigated. Another interesting research question could be to look at the correlation between forecast of renewable power generation and the day-ahead prices on the one hand and actual values and intra-day prices on the other hand. How strong is the influence of forecasting errors for wind and solar power generation?

Bibliography

[1] Augsburger Allgemeine. *Mega-Stromtrasse: Statt Meitingen soll Gundremmingen das Ziel sein.* Augsburger Allgemeine. URL https://www.augsburger-allgemeine.de/bayern/Mega-Stromtrasse-Statt-Meitingen-soll-Gundremmingen-das-Ziel-sein-id31884712.html. Visited: 24.06.2020.

[2] M. Anvari, G. Lohmann, M. Wächter, P. Milan, E. Lorenz, D. Heinemann, M. Reza Rahimi Tabar, and J. Peinke. Short term fluctuations of wind and solar power systems. *New Journal of Physics*, 18, 2016. URL https://doi.org/10.1088/1367-2630/18/6/063027.

[3] BMU. *Treibhausgas-Emissionen in Deutschland.* Bundesministerium für Umwelt, Naturschutz und nukleare Sicherheit (BMU). URL https://www.umweltbundesamt.de/daten/klima/treibhausgas-emissionen-in-deutschland. Visited: 19.06.2020.

[4] BMWi. *Erneuerbare Energien in Zahlen.* Bundesministerium für Wirtschaft und Energie (BMWi), 2019. URL https://www.bmwi.de/Redaktion/DE/Publikationen/Energie/erneuerbare-energien-in-zahlen-2018.html. Visited: 19.06.2020.

[5] BMWi. *Mehr Strom vom Meer - 20 Gigawatt Offshore-Windenergie bis 2030 realisieren.* Bundesministerium für Wirtschaft und Energie (BMWi), 2020. URL https://www.bmwi.de/Redaktion/DE/Downloads/M-O/offshore-vereinbarung-mehr-strom-vom-meer.pdf. Visited: 19.06.2020.

[6] BMWi. *Zeitreihen zur Entwicklung der erneuerbaren Energien in Deutschland.* Bundenministerium für Wirtschaft und Energie (BMWi), 2020. URL https://www.erneuerbare-energien.de/EE/Redaktion/DE/Downloads/zeitreihen-zur-entwicklung-der-erneuerbaren-energien-in-deutschland-1990-2019.pdf?__blob=publicationFile&v=26. Visited: 02.08.2020.

[7] M. Bonamente. *Statistics and Analysis of Scientific Data.* Springer Science and Business Media New York, 2 edition, 2013. ISBN 978-1-4939-6570-0. URL https://doi.org/10.1007/978-1-4939-6572-4.

[8] R. Bono, J. Arnau, R. Alarcón, and M.J. Blanca. Bias, Precision, and Accuracy of Skewness and Kurtosis Estimators for Frequently Used Continuous Distributions. *Symmetry*, 12(1):19, 2020. URL https://doi.org/10.3390/sym12010019.

[9] P.J. Brockwell and R.A. Davis. *Introduction to Time Series and Forecasting*. Springer International Publishing Switzerland, 3 edition, 2016. ISBN 978-3-319-29852-8. URL https://doi.org/10.1007/978-3-319-29854-2.

[10] T. Brown. *Energy System Modelling Course at KIT*. 2020. URL https://nworbmot.org/courses/esm-2020/. Visited: 28.07.2020.

[11] Bundesnetzagentur. *Warum brauchen wir den Netzausbau?* URL https://www.netzausbau.de/wissenswertes/warum/de.html. Visited: 24.06.2020.

[12] Bundesnetzagentur. *Bedarfsermittlung 2024 - Bestätigung Netzentwicklungsplan Strom (Zieljahr 2024)*. 2015. URL https://www.netzentwicklungsplan.de/sites/default/files/paragraphs-files/NEP_2024_Bestaetigung.pdf. Visited: 07.07.2020.

[13] S. Collins, P. Deane, B. Ó Gallachóir, S. Pfenninger, and I. Staffell. Impacts of Inter-annual Wind and Solar Variations on the European Power System. *Joule*, 2: 2076–2090, 2018. URL https://doi.org/10.1016/j.joule.2018.06.020.

[14] J.D. Cryer and K.-S. Chan. *Time Series Analysis - With Application in R*. Springer Science and Business Media, 2 edition, 2008. ISBN 978-0-387-75958-6. URL https://doi.org/10.1007/978-0-387-75959-3.

[15] D. Barbosa de Alencar, C. de Mattos Affonso, R.C. Limão de Oliveira, J.L. Moya Rodríguez, J.C. Leite, and J.C. Reston Filho. Different Models for Forecasting Wind Power Generation: Case Study. *Energies*, 10:1976, 2017. URL https://doi.org/10.3390/en10121976.

[16] H. Dehling and B. Haupt. *Einführung in die Wahrscheinlichkeitstheorie und Statistik*. Springer, Berlin Heidelberg New York, 2 edition, 2004. ISBN 978-3-540-20380-3. URL https://doi.org/10.1007/3-540-35117-5.

[17] S.J. Devlin, R. Gnanadesikan, and J.R. Kettenring. Robust estimation and outlier detection with correlation coefficients. *Biometrika*, 62(3):531–545, 1975. URL https://doi.org/10.1093/biomet/62.3.531.

[18] D.R. Drew, P.J. Coker, H.C. Bloomfield, D.J. Brayshaw, J.F. Barlow, and A. Richards. Sunny windy sundays. *Renewable Energy*, 138:870–875, 2019. URL https://doi.org/10.1016/j.renene.2019.02.029.

[19] P. Elsner, B. Erlach, M. Fischedick, B. Lunz, and D.U. Sauer. *Flexibilitätskonzepte für die Stromversorgung 2050: Technologien – Szenarien – Systemzusammenhänge (Analyse aus der Schriftenreihe Energiesysteme der Zukunft)*. 2015. URL https://www.acatech.de/wp-content/uploads/2018/03/ESYS_Analyse_Flexibilitaetskonzepte.pdf. Visited: 15.06.2020.

[20] EPEX SPOT. *Trading Products*. European Power Exchange SE. URL https://www.epexspot.com/en/tradingproducts. Visited: 28.07.2020.

[21] European Union. *Richtlinie 2009/28/EG*. 2009. URL https://eur-lex.europa.eu/legal-content/DE/TXT/PDF/?uri=uriserv:OJ.L_.2009.140.01.0016.01.DEU. Visited: 28.06.2020.

[22] F. Genoese, M. Genoese, and M. Wietschel. Occurrence of negative prices on the German spot market for electricity and their influence on balancing power markets. *2010 7th International Conference on the European Energy Market*, pages 1–6, 2010. URL https://doi.org/10.1109/EEM.2010.5558703.

[23] H.-O. Georgii. *Stochastik*. Walter de Gruyter, Berlin, New York, 4 edition, 2009. ISBN 978-3-11-021526-7. URL https://doi.org/10.1515/9783110215274.

[24] L. Rydin Gorjão, M. Anvari, H. Kantz, C. Beck, D. Witthaut, M. Timme, and B. Schäfer. Data-Driven Model of the Power-Grid Frequency Dynamics. *IEEE Access*, 8:43082–43097, 2020. URL https://doi.org/10.1109/ACCESS.2020.2967834.

[25] Y. He, M. Hildmann, F. Herzog, and G. Andersson. Modeling the Merit Order Curve of the European Energy Exchange Power Market in Germany. *IEEE Transactions on Power Systems*, 28(3):3155–3164, 2013. URL https://doi.org/10.1109/TPWRS.2013.2242497.

[26] D. Heide, L. von Bremen, M. Greiner, C. Hoffmann, M. Speckmann, and S. Bofinger. Seasonal optimal mix of wind and solar power in a future, highly renewable Europe. *Renewable Energy*, 35(11):2483–2489, 2010. URL https://doi.org/10.1016/j.renene.2010.03.012.

[27] S. Heidorn. *Dank Windpower: Deutschland verschenkt Strom über Weihnachten*. TrendsDerZukunft.de - Heidorn GmbH. URL https://www.trendsderzukunft.de/dank-windpower-deutschland-verschenkt-strom-ueber-weihnachten/. Visited: 31.07.2020.

[28] B. Hengst. *Bayerns Angst vor der Monstertrasse*. Spiegel. URL https://www.spiegel.de/politik/deutschland/energiewende-seehofer-kuendigt-kampf-gegen-gleichstromtrasse-an-a-962682.html. Visited: 24.06.2020.

[29] O. Hoegh-Guldberg, P.J. Mumby, A.J. Hooten, R.S. Steneck, P. Greenfield, E. Gomez, C.D. Harvell, P.F. Sale, A.J. Edwards, K. Caldeira, N. Knowlton, C.M. Eakin, R. Iglesias-Prieto, N. Muthiga, R.H. Bradbury, A. Dubi, and M.E. Hatziolos. Coral Reefs Under Rapid Climate Change and Ocean Acidification. *Science*, 318(5857):1737–1742, 2007. URL https://doi.org/10.1126/science.1152509.

[30] IEA. *Wind Energy Annual Report*. International Energy Agency (IEA), Paris, 2006. URL https://community.ieawind.org/HigherLogic/System/DownloadDocumentFile.ashx?DocumentFileKey=e01252b5-7ad6-ccbe-aad4-4c61d8f898f8&forceDialog=0. Visited: 24.06.2020.

[31] IEA. *Offshore Wind Outlook 2019*. International Energy Agency (IEA), Paris, 2019. URL https://www.iea.org/reports/offshore-wind-outlook-2019. Visited: 25.06.2020.

[32] IEA. *Renewables Information: Overview*. International Energy Agency (IEA), Paris, 2019. URL https://www.iea.org/reports/renewables-information-2019. Visited: 27.06.2020.

[33] IEA. *Renewables 2019 - Market analysis and forecast from 2019 to 2024*. International Energy Agency (IEA), Paris, 2019. URL https://www.iea.org/reports/renewables-2019. Visited: 27.06.2020.

[34] IEA. *World Energy Outlook 2019*. International Energy Agency (IEA), Paris, 2019. URL https://www.iea.org/reports/world-energy-outlook-2019. Visited: 27.06.2020.

[35] L. Igual and S. Seguí. *Introduction to Data Science - A Python Approach to Concepts, Techniques and Applications*. Springer International Publishing Switzerland, 1 edition, 2017. ISBN 978-3-319-50016-4. URL https://doi.org/10.1007/978-3-319-50017-1.

[36] IPCC. *Climate Change*. Intergovernmental Panel on Climate Change (IPCC), 1990. URL https://www.ipcc.ch/report/ar1/wg1/. Visited: 19.06.2020.

[37] IPCC. *Renewable Energy Sources and Climate Change Mitigation*. Intergovernmental Panel on Climate Change (IPCC), 2012. URL https://www.ipcc.ch/report/renewable-energy-sources-and-climate-change-mitigation/. Visited: 26.06.2020.

[38] IPCC. *Climate Change 2013: The Physical Science Basis*. Intergovernmental Panel on Climate Change (IPCC), 2013. URL https://www.ipcc.ch/report/ar5/wg1/. Visited: 19.06.2020.

[39] IPCC. *Climate Change 2014: Mitigation of Climate Change*. Intergovernmental Panel on Climate Change (IPCC), 2014. URL https://www.ipcc.ch/report/ar5/wg3/. Visited: 19.06.2020.

[40] IPCC. *Global Warming of 1.5°C*. Intergovernmental Panel on Climate Change (IPCC), 2018. URL https://www.ipcc.ch/sr15/. Visited: 19.06.2020.

[41] IRENA. *Renewable Power Generation Costs in 2018*. International Renewable Energy Agency (IRENA), 2019. URL https://www.irena.org/publications/2019/May/Renewable-power-generation-costs-in-2018. Visited: 15.06.2020.

[42] D.N. Joanes and C.A. Gill. Comparing Measures of Sample Skewness and Kurtosis. *Journal of the Royal Statistical Society: Series D (The Statistician)*, 47(1):183–189, 1998. URL https://www.jstor.org/stable/2988433. Visited: 25.07.2020.

[43] M.E. Johnson, G.L. Tietjen, and R.J. Beckman. A New Family of Probability Distributions With Applications to Monte Carlo Studies. *Journal of the American Statistical Association*, 75(370):276–279, 1980. URL http://www.jstor.org/stable/2287446. Visited: 04.06.2020.

[44] F. Kaiser, J. Strake, and D. Witthaut. Collective effects of link failures in linear flow networks. *New Journal of Physics*, 22(1), 2020. URL https://doi.org/10.1088/1367-2630/ab6793.

[45] M.G. Kendall. *Rank Correlation Methods*. Griffin, London, 4 edition, 1970. ISBN 0-85264-199-0.

[46] A. Knaut and S. Paulus. *Hourly price elasticity pattern of electricity demand in the German day-ahead market*. Technical report, EWI Working Paper, 2016. URL http://hdl.handle.net/10419/144865. Visited: 28.07.2020.

[47] U. Krengel. *Einführung in die Wahrscheinlichkeitstheorie und Statistik*. Vieweg, Wiesbaden, 8 edition, 2005. ISBN 3-8348-0063-5. URL https://doi.org/10.1007/978-3-663-09885-0.

[48] B. Kroposki, B. Johnson, Y. Zhang, V. Gevorgian, P. Denholm, B.-M. Hodge, and B. Hannegan. Achieving a 100% Renewable Grid: Operating Electric Power Systems with Extremely High Levels of Variable Renewable Energy. *IEEE Power and Energy Magazine*, 15(2):61–73, 2017. URL https://doi.org/10.1109/MPE.2016.2637122.

[49] V. Lagendijk and E. van der Vleuten. *Inventing Electrical Europe: Interdependencies, Borders, Vulnerabilities*, pages 62–101. In: P. Högselius, A. Hommels, A. Kaijser, E. van der Vleuten(eds). The Making of Europe's Critical Infrastructure. Palgrave Macmillan, London, 2013. URL https://doi.org/10.1057/9781137358738_3.

[50] N. Ohlendorf and W.P. Schill. Frequency and duration of low-wind-power events in Germany. *Environmental Research Letters*, 2020. URL https://doi.org/10.1088/1748-9326/ab91e9.

[51] T. Pesch, H.-J. Allelein, and J.-F. Hake. Impacts of the transformation of the German energy system on the transmission grid. *The European Physical Journal Special Topics*, 223:2561–2575, 2014. URL https://doi.org/10.1140/epjst/e2014-02214-y.

[52] B. Rajendran. *Review of Noise in Semiconductor Devices and Modeling of Noise in Surrounding Gate MOSFET*. 2001. URL https://web.archive.org/web/20060414084209/http://www.stanford.edu/~bipin/research/Noise.pdf. Visited: 05.06.2020.

[53] REN21. *Renewables 2020 Global Status Report*. Renewable Energy Policy Network for the 21st Century (REN21), Paris, 2020. URL https://www.ren21.net/wp-content/uploads/2019/05/gsr_2020_full_report_en.pdf.

[54] S.M. Ross. *Stochastic Processes*. John Wiley and Sons, New York, Chichester, Brisbane, Toronto, Singapore, 2 edition, 1996. ISBN 0-471-12062-6.

[55] B. Schäfer, D. Witthaut, M. Timme, and V. Latora. Dynamically induced cascading failures in power grids. *Nature Communications*, 9(1975), 2018. URL https://doi.org/10.1038/s41467-018-04287-5.

[56] C. Spearman. The Proof and Measurement of Association between Two Things. *American Journal of Psychology*, 15(1):72–101, 1904. URL https://doi.org/10.2307/1412159.

[57] Statkraft. *Negative Preise am Beispiel 8. Mai 2016*. Statkraft Markets GmbH. URL https://www.statkraftdirektvermarktung.de/news/blog/archive/negative-preise-am-beispiel-8.-mai-2016/. Visited: 31.07.2020.

[58] G. Strbac. Demand side management: Benefits and challenges. *Energy Policy*, 36 (12):4419–4426, 2008. URL https://doi.org/10.1016/j.enpol.2008.09.030.

[59] UNFCCC. *The Paris Agreement*. The 21st Conference of the Parties to the United Nations Framework, Convention on Climate Change (UNFCCC), 2015. URL http://unfccc.int/paris_agreement/items/9485.php. Visited: 19.06.2020.

[60] F. Wagner. Electricity by intermittent sources: An analysis based on the German situation 2012. *The European Physical Journal Plus*, 129(20), 2014. URL https://doi.org/10.1140/epjp/i2014-14020-8.

[61] L. Wasserman. *All of Statistics - A concise Course in Statistical Inference*. Springer Science and Business Media New York, 2 edition, 2004. ISBN 978-1-4419-2322-6. URL https://doi.org/10.1007/978-0-387-21736-9.

[62] J. Weber, M. Reyers, C. Beck, M. Timme, J. G. Pinto, D. Witthaut, and B. Schäfer. Wind Power Persistence Characterized by Superstatistics. *Scientific Reports*, 9(1): 1–15, 2019. URL https://doi.org/10.1038/s41598-019-56286-1.

[63] P.H. Westfall. Kurtosis as Peakedness, 1905–2014. R.I.P. *The American Statistician*, 68(3):191–195, 2014. URL https://doi.org/10.1080/00031305.2014.917055.

[64] WetterOnline. *Rückblick Dezember 2016 - Extrem trocken und sonnig*. WetterOnline Meteorologische Dienstleistungen GmbH, 2016. URL https://www.wetteronline.de/wetterrueckblick/rueckblick-dezember-2016-extrem-trocken-und-sonnig-2016-12-29-rd. Visited: 05.08.2020.

[65] J. Wohland. *Impacts of climate variability and climate change on renewable power generation*. PhD thesis, Universität zu Köln, 2019. URL https://kups.ub.uni-koeln.de/9852/. Visited: 15.06.2020.

[66] J. Wohland, M. Reyers, C. Märker, and D. Witthaut. Natural wind variability triggered drop in German redispatch volume and costs from 2015 to 2016. *PLOS One*, 13, 2018. URL https://doi.org/10.1371/journal.pone.0190707.

[67] J. Wohland, N.A. Omrani, N. Keenlyside, and D. Witthaut. Significant multidecadal variability in German wind energy generation. *Wind Energy Science*, 4(3):515–526, 2019. URL https://doi.org/10.5194/wes-4-515-2019.

A Appendix

A.1 Data Availability

Solar power generation data are available at www.netztransparenz.de. Wind power generation data are available at the websites of the German network operators www.50hertz.com, www.amprion.net, www.tennet.eu, www.transnetbw.de. Load data are available from ENTSO-E www.entsoe.eu. Raw data for the price analysis is bought from the European Power Exchange (EPEX SPOT).

A.2 Additional Figures

A.2.1 Renewable Energy Systems

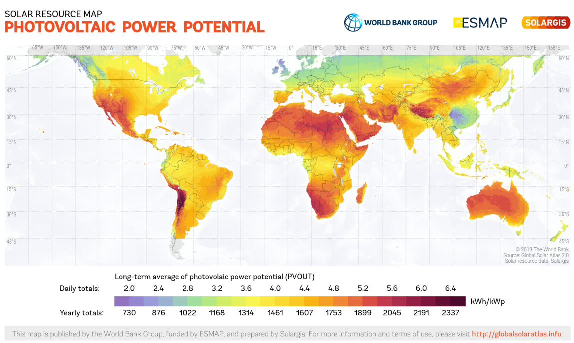

(a) This map shows the world wide photovoltaic power potential.
(Source: World Bank Group, *Photovoltaic Power Potential*, https://globalsolaratlas.info/download/world, visited: 07.07.2020)

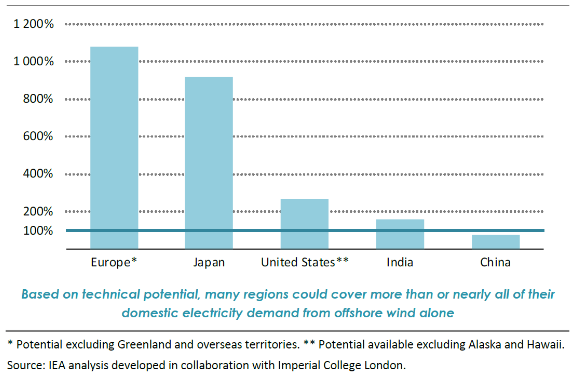

(b) This figure shows the ratio of technical potential to meet the domestic electricity demand with offshore wind power.
(Source: IEA, *Offshore Wind Outlook* [31], p. 50, fig. 26. All rights reserved.)

A.2.2 Influencing Factors of Electricity Prices

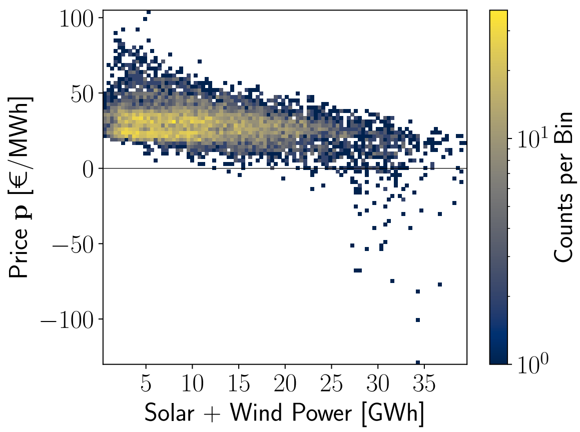

Figure A.2: Equal to figure 4.1 the generation of variable renewable energy is plotted against the wholesale electricity price. The correlation between electricity prices and renewable energy generation is quantified with the correlation measures $\tau = -0.2210$, $\rho = -0.3249$, $r = -0.4174$.

A.2.3 Time Series

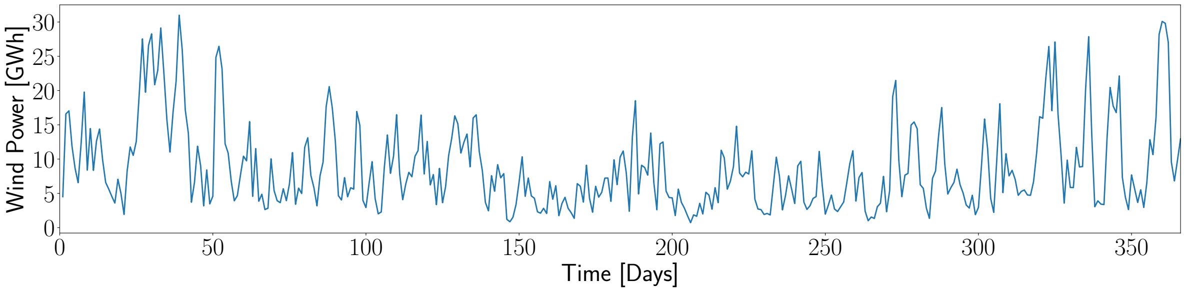

(a) The daily mean wind power generation is plotted against time in days. Light seasonal influences can be observed.

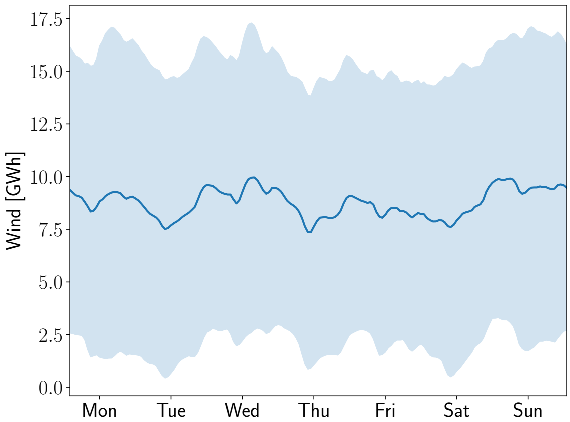

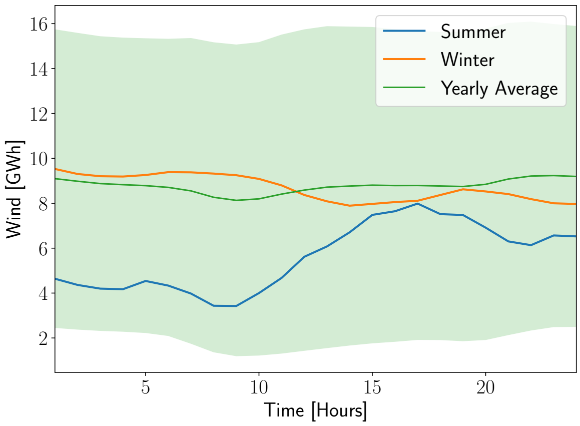

(b) The weekly of wind power generation is created by calculating the average wind power generation for each hour of the week over the whole year. The light blue area marks the standard deviation. There are no strong visible differences in the patterns between and within the days, but the variance is significant.

(c) The daily wind power trajectory for one day is created by taking the average wind power generation for each hour of the day over the whole year. The light green area marks the standard deviation. For summer and winter the development of wind power generation is plotted for one day each. The plotted summer's day is the 05.08.2016, the winter's day is the 05.01.2016.

Figure A.3: The wind power generation of 2016 shows huge deviations between days and seasons. The generation is mostly stochastic with little seasonal influence, leading to the wind power generation being a slightly higher in winter that it is in summer. It is mostly independent of the day or the time of day.

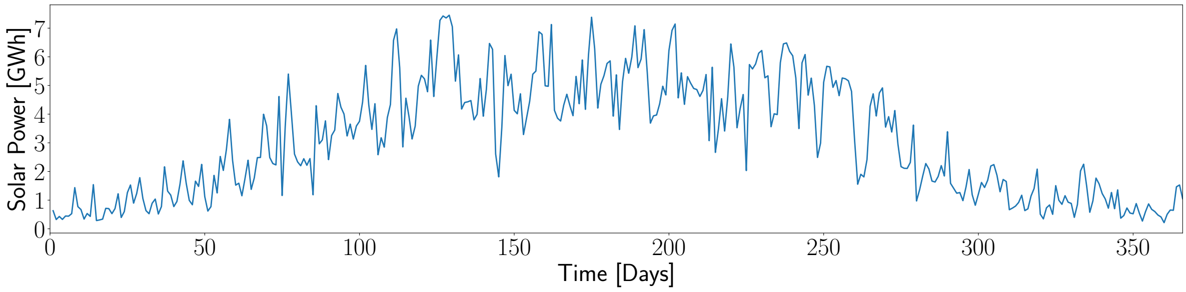

(a) The daily mean solar power generation is plotted against time in days. Strong seasonal influences can be observed.

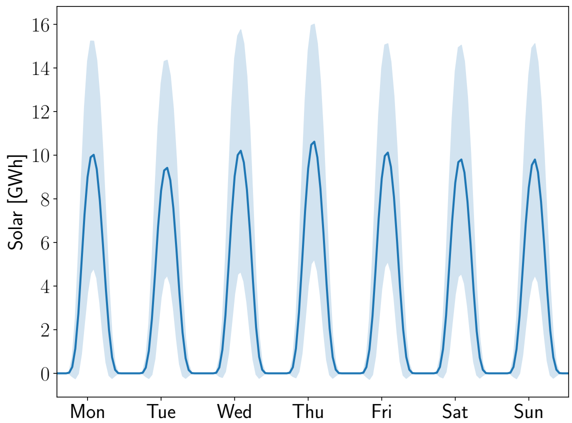

(b) The weekly solar power generation is created by calculating the average solar power generation for each hour of the week over the whole year. The light blue area marks the standard deviation. Changing patterns between the days are not visible.

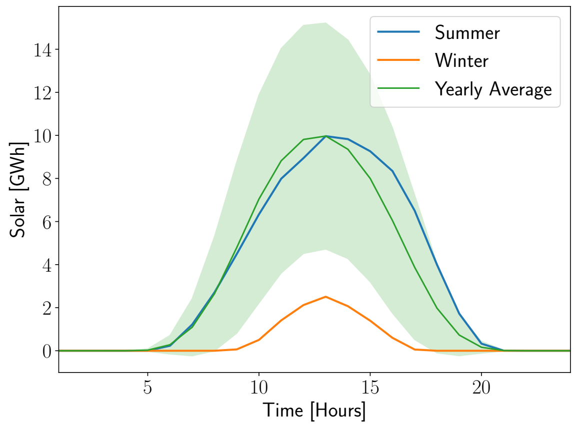

(c) The daily solar power trajectory for one day is created by calculating the average solar power generation for each hour of the day over the whole year. The light green area marks the standard deviation. For summer and winter the development of wind power generation is plotted for one day each. The plotted summer's day is the 05.08.2016, the winter's day is the 05.01.2016.

Figure A.4: Solar power generation for 2016 shows a high dependence on seasons and the time of day, as it dependents on sunshine. The solar power generation in remarkably higher in summer and only exists during daylight with a high standard deviation between the days.

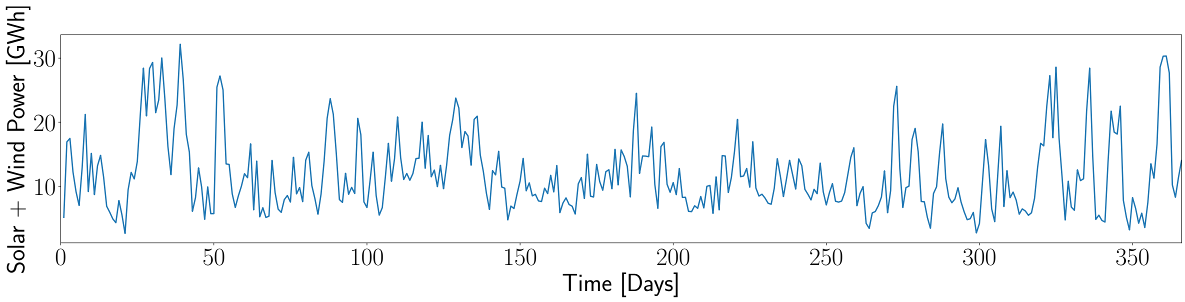

(a) The daily mean renewable power generation from wind and solar (variable renewable energy) is plotted against time in days.

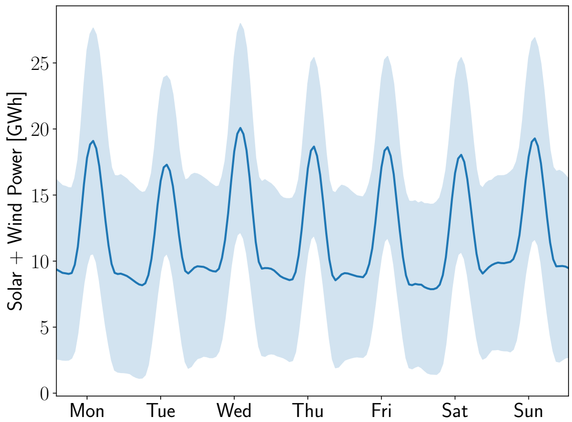

(b) The weekly development of variable renewable energy is created by calculating the average variable renewable power generation for each hour of the week over the whole year. The light blue area marks the standard deviation.

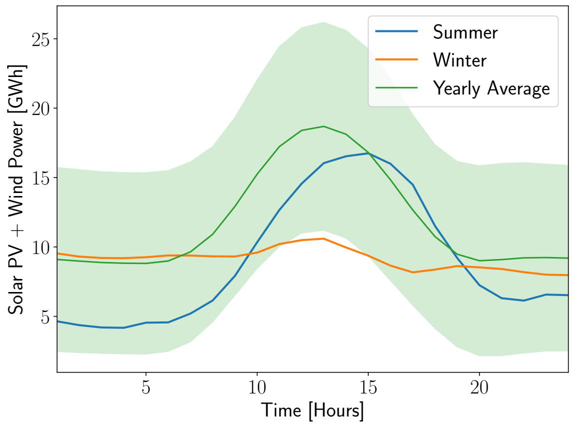

(c) The daily variable renewable power trajectory is created by calculating the average variable renewable power generation for each hour of the day over the whole year. The light green area marks the standard deviation. For summer and winter the development of wind power generation is plotted for one day each. The plotted summer's day is the 05.08.2016, the winter's day is the 05.01.2016.

Figure A.5: Variable renewable energy generation for 2016 shows huge standard deviations. The weekly average as well as the daily average are mostly dominated by solar power generation, because wind power generation is equally distributed over one day and between the days of a week and therefore only provides an offset.

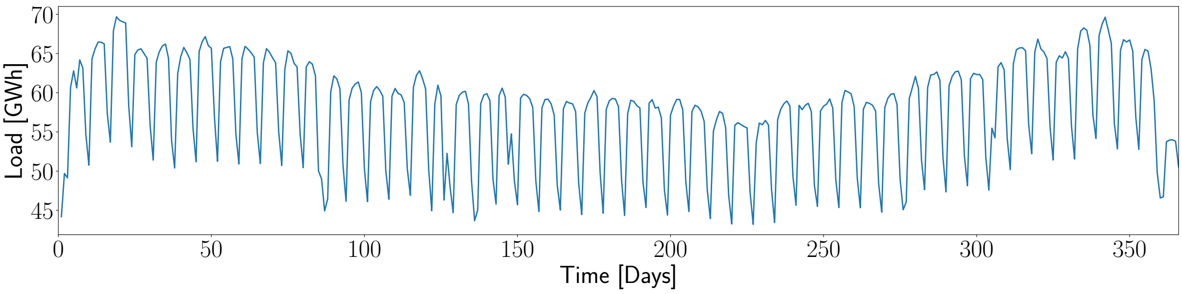

(a) The daily mean load is plotted against time in days. Weekends and public holidays are marked by local minima.

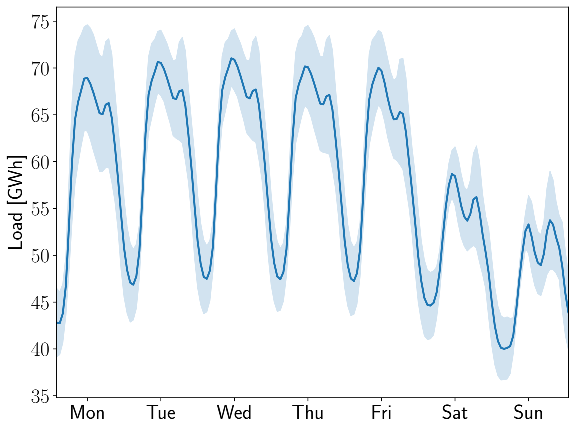

(b) The weekly development of load is created by calculating the average load for each hour of the week over the whole year. The light blue area marks the standard deviation.

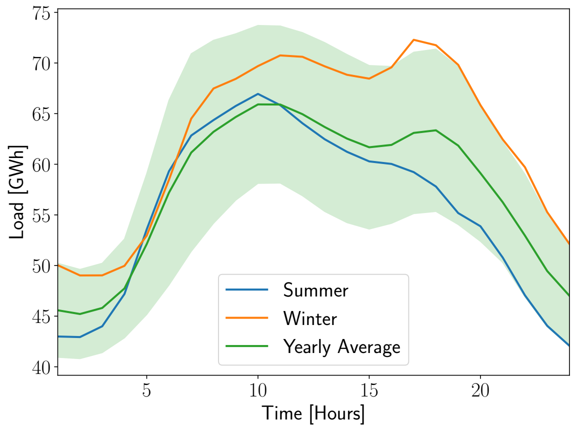

(c) The daily load trajectory is created by calculating the average load for each hour of the day over the whole year. The light green area marks the standard deviation. For summer and winter the development of the load is plotted for one day each. The plotted summer's day is the 05.08.2016, the winter's day is the 05.01.2016.

Figure A.6: The load trajectory is mostly dominated by the time of day. The load peaks in the morning and in the evening and is significantly lower during the night. It drops on weekends and public holidays. Slight seasonal patterns can be observed.

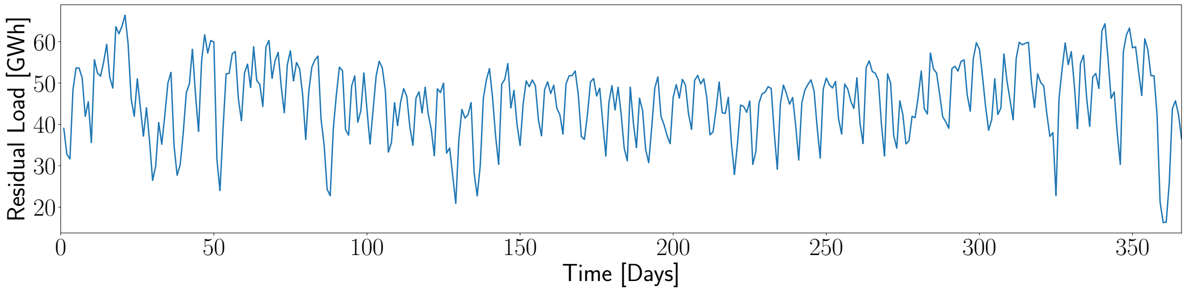

(a) The daily mean residual load is plotted against time in days. Weekends and public holidays are marked by local minima.

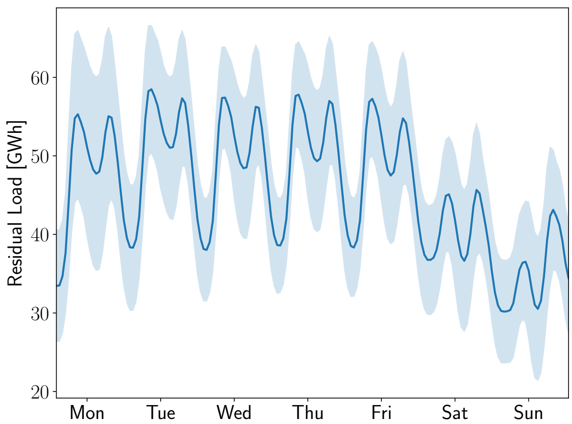

(b) The weekly development of residual load is created by calculating the average residual load for each hour of the week over the whole year. The light blue area marks the standard deviation.

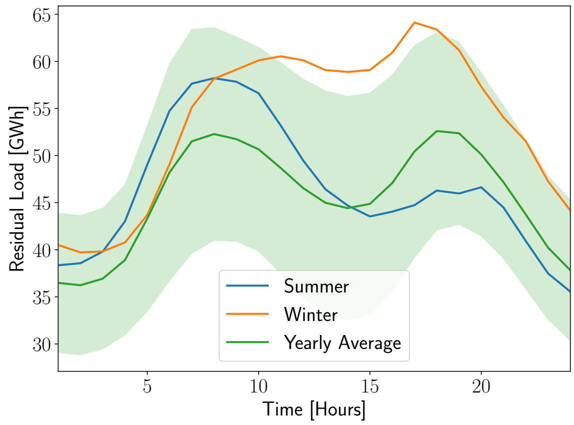

(c) The daily residual load trajectory is created by calculating the average residual load for each hour of the day over the whole year. The light green area marks the standard deviation. For summer and winter the development of the residual load is plotted for one day each. The plotted summer's day is the 05.08.2016, the winter's day is the 05.01.2016.

Figure A.7: The residual load trajectory is mostly dominated by the time of day. The load peaks in the morning and in the evening and is significantly lower during the night. It drops on weekends and public holidays. Slight seasonal patterns can be observed.

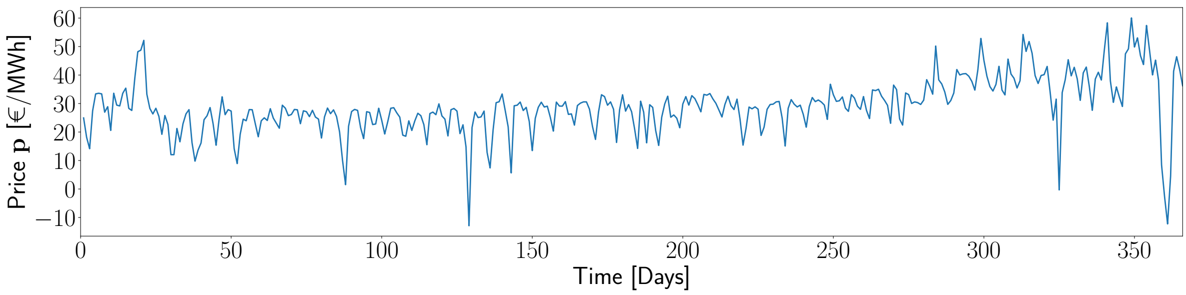

(a) The daily mean price is plotted against time in days.

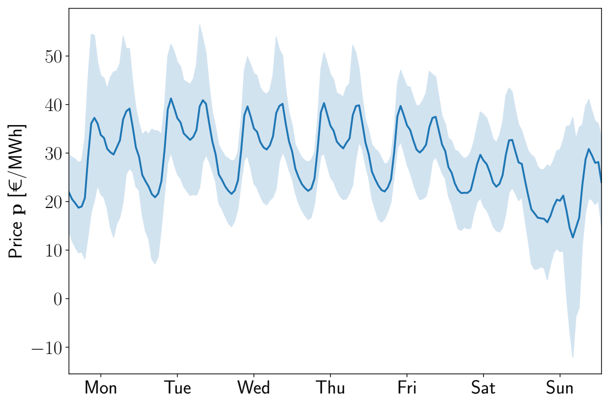

(b) The weekly development of the price is created by calculating the average price for each hour of the week over the whole year. The light blue area marks the standard deviation.

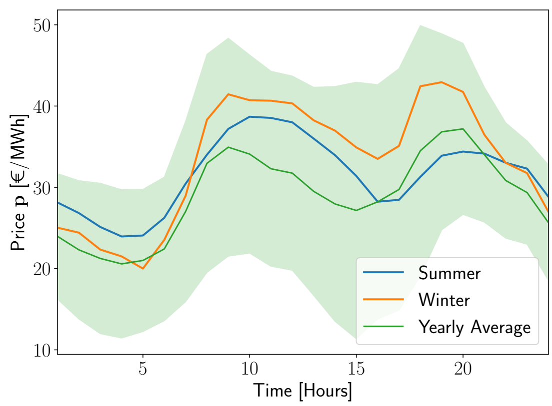

(c) The daily price trajectory is created by taking the average price for each hour of the day over the whole year. For summer and winter the development of wind power generation is plotted for one day each. The light green area marks the standard deviation. The plotted summer's day is the 05.08.2016, the winter's day is the 05.01.2016.

Figure A.8: Equally to the load the wholesale electricity prices for 2016 are mostly dominated by the time of day. The price peaks in the morning and in the evening and is significantly lower during the night. It drops on weekends, even thought the decrease is smaller, than it is for the load. Compared to the load, wholesale electricity prices show a much higher standard deviation.

A.2.4 Exponential Maximum-Likelihood Fit of Waiting Times

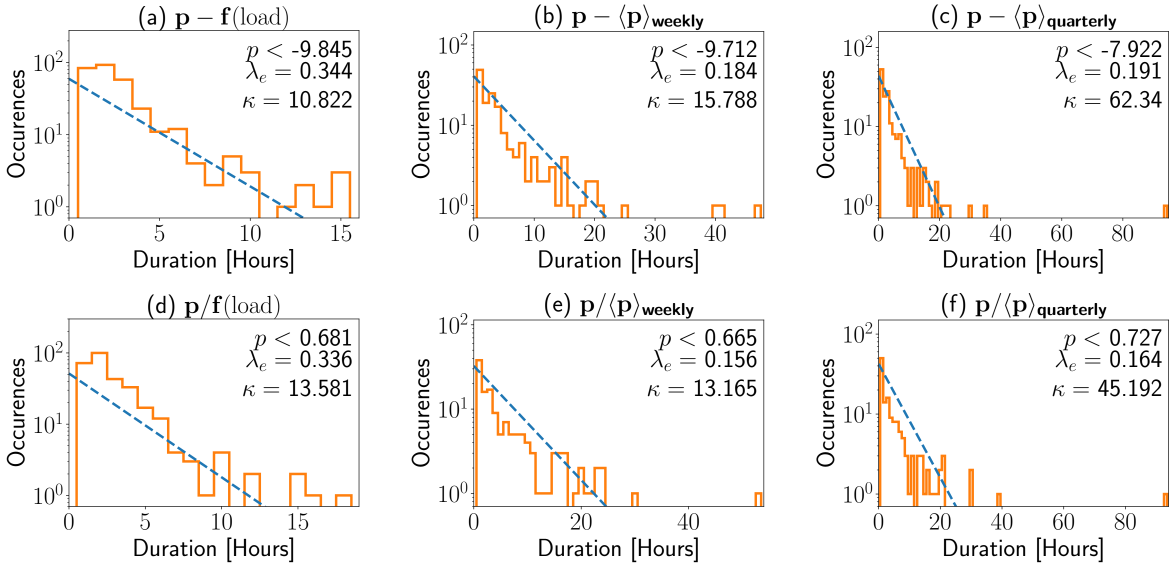

Figure A.9: Kurtosis κ and histogram of the duration of periods in which the normalized price $p(t)$ is lower than the 50% quantil, together with an exponential maximum-likelihood fit with exponent λ_e.

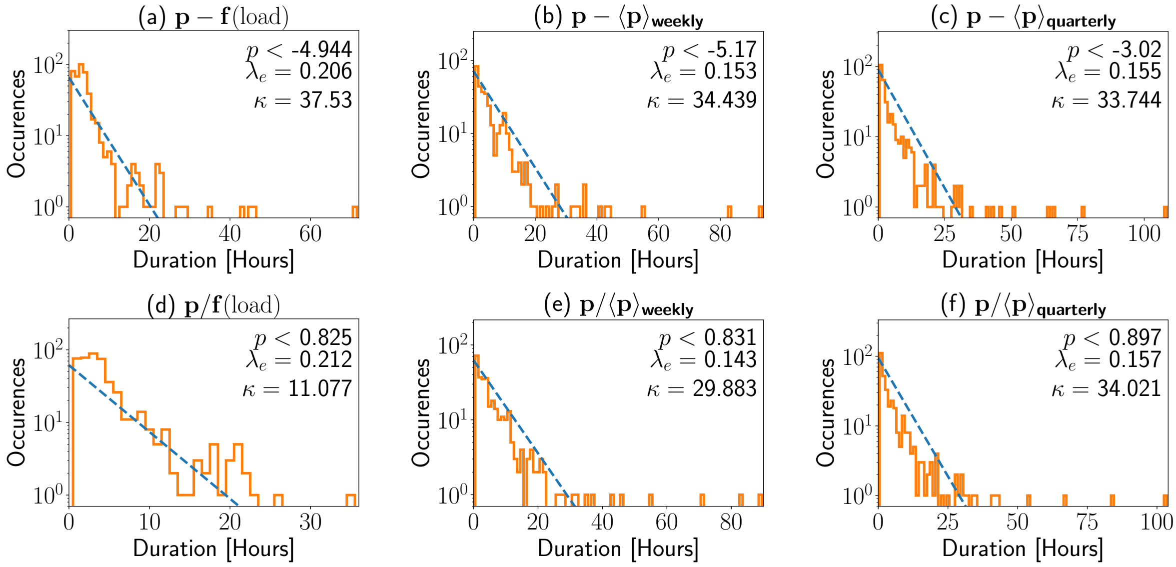

Figure A.10: Kurtosis κ and histogram of the duration of periods in which the normalized price $p(t)$ is lower than the 25% quantil, together with an exponential maximum-likelihood fit with exponent λ_e.

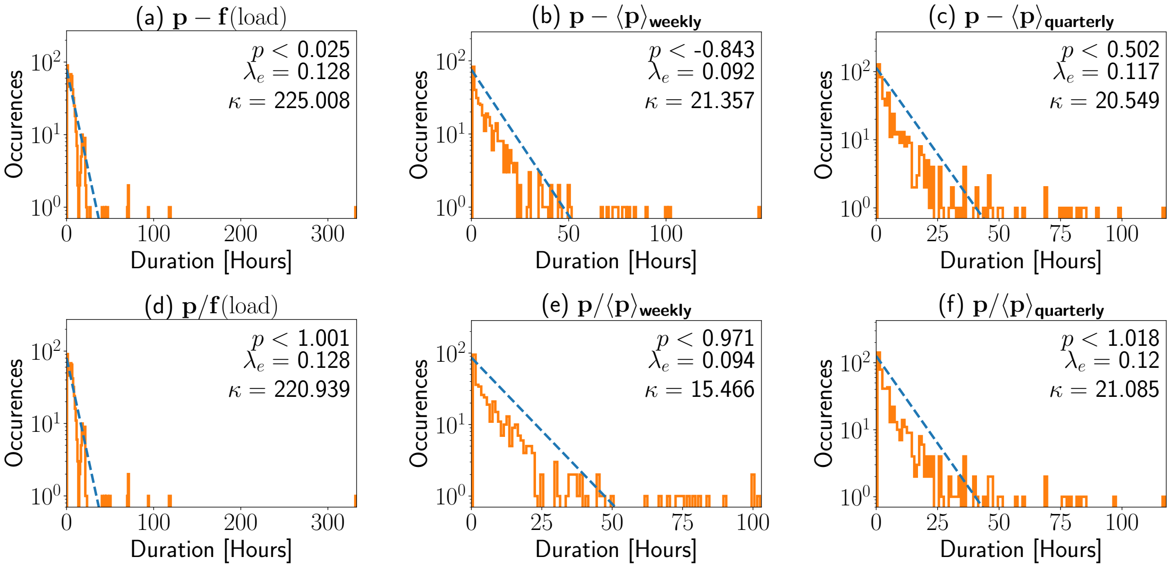

Figure A.11: Kurtosis κ and histogram of the duration of periods in which the normalized price $p(t)$ is lower than the 50% quantil, together with an exponential maximum-likelihood fit with exponent λ_e.

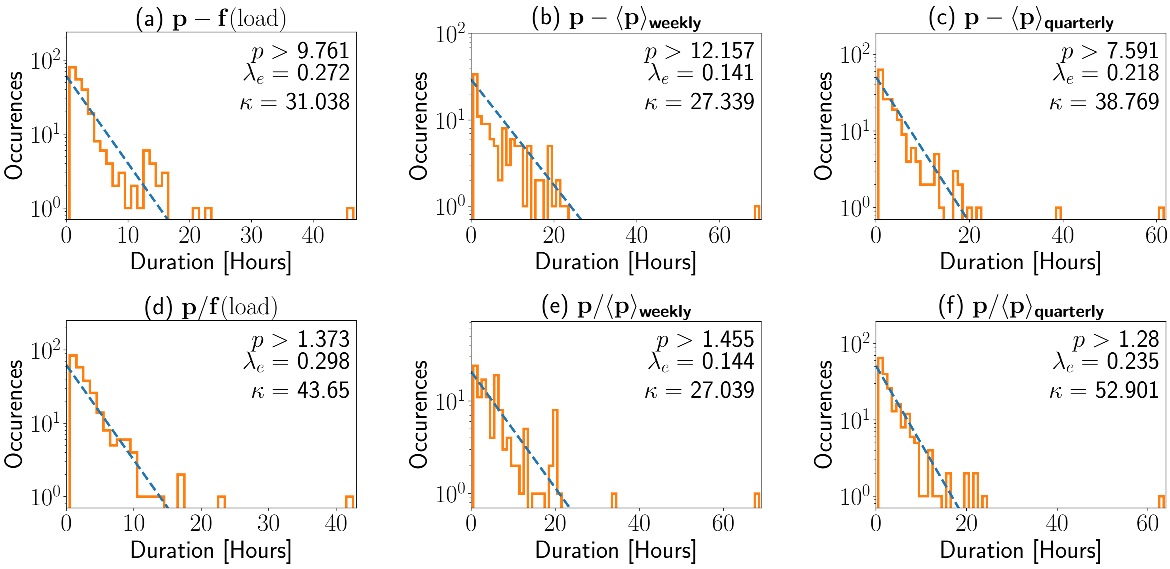

Figure A.12: Kurtosis κ and histogram of the duration of periods in which the normalized price $p(t)$ is lower than the 90% quantil, together with an exponential maximum-likelihood fit with exponent λ_e.

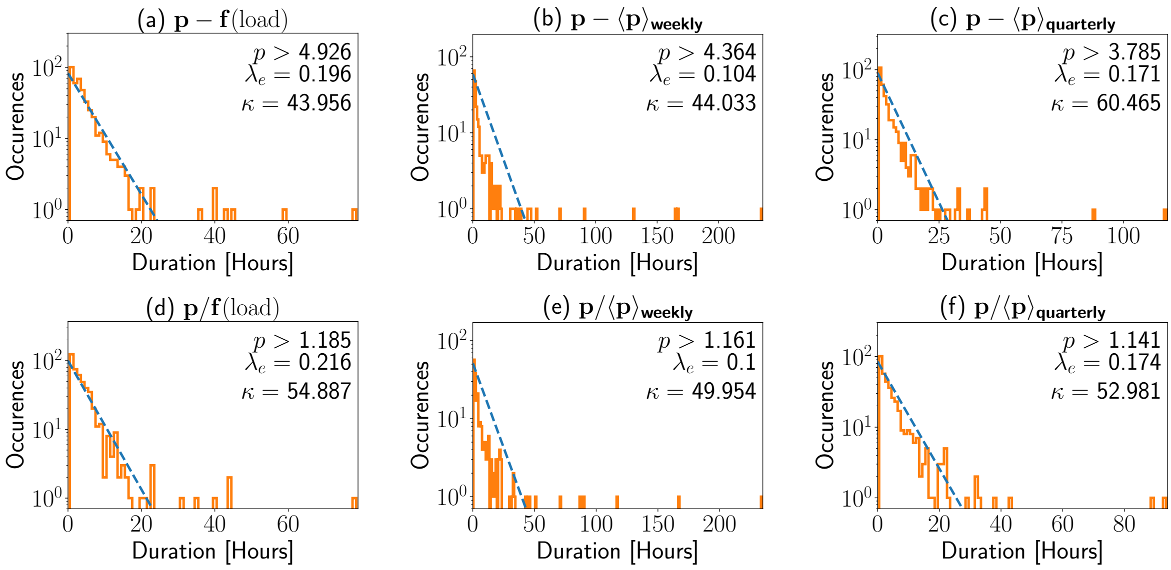

Figure A.13: Kurtosis κ and histogram of the duration of periods in which the normalized price $p(t)$ is lower than the 75% quantil, together with an exponential maximum-likelihood fit with exponent λ_e.

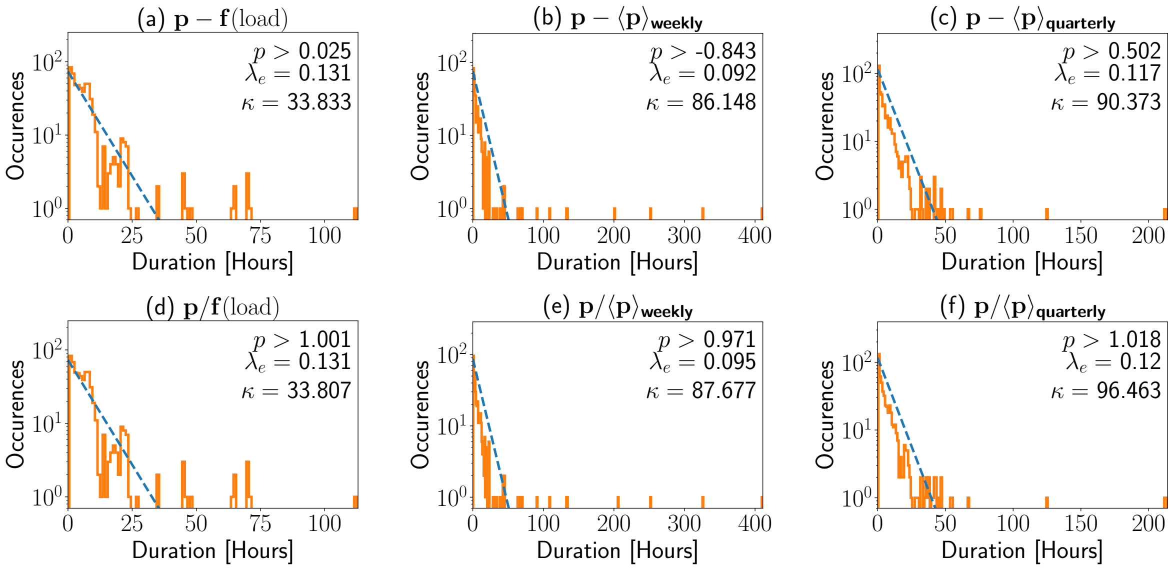

Figure A.14: Kurtosis κ and histogram of the duration of periods in which the normalized price $p(t)$ is higher than the 50% quantil, together with an exponential maximum-likelihood fit with exponent λ_e.

A.2.5 Kurtosis vs. Threshold

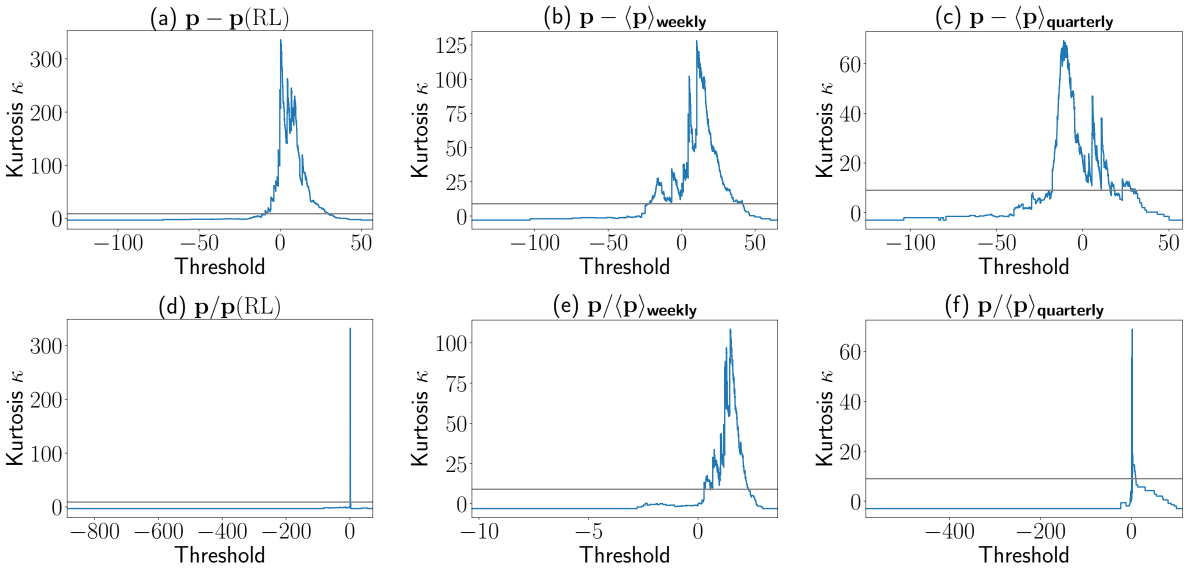

Figure A.15: Kurtosis for the persistence of the normalized wholesale electricity prices $p(t)$ being lower than the threshold plotted for the whole range of possible thresholds.

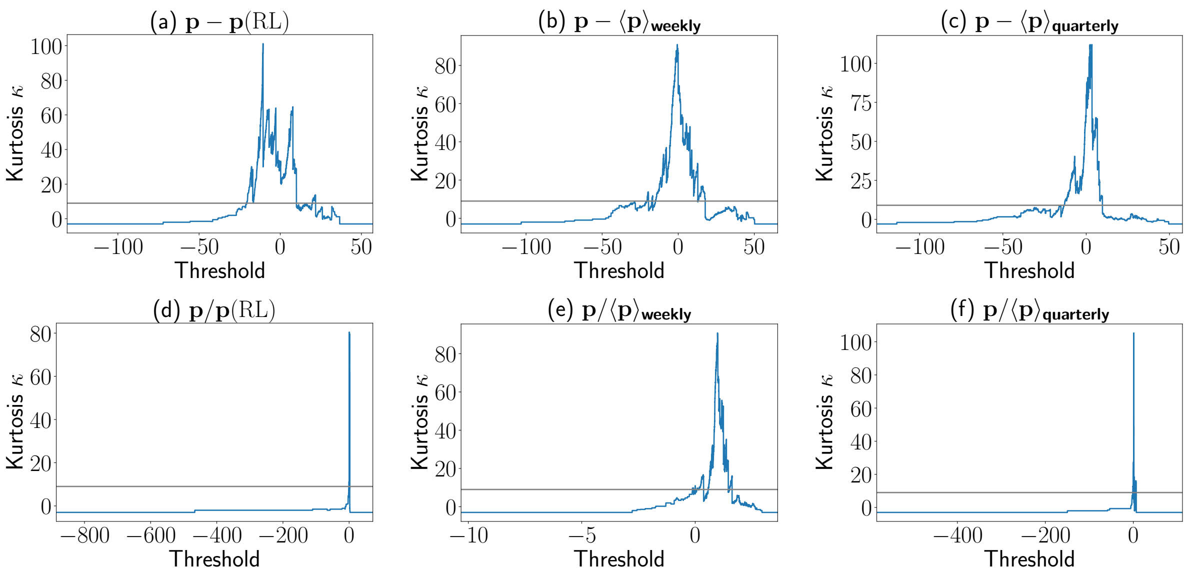

Figure A.16: Kurtosis for the persistence of normalized wholesale electricity prices $p(t)$ being higher than the threshold plotted for the whole range of possible thresholds.

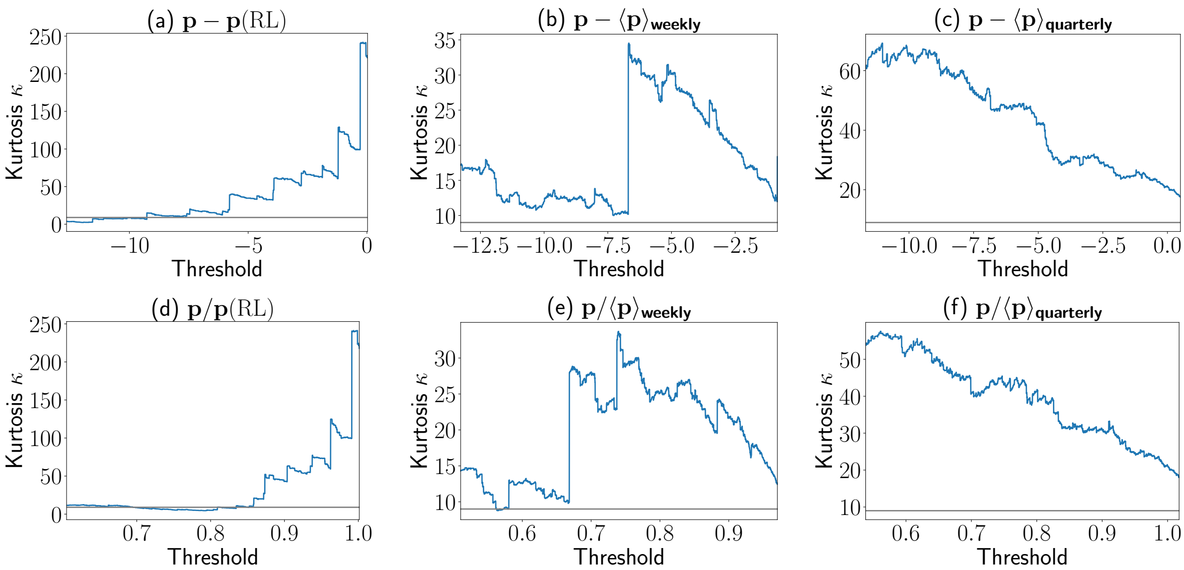

Figure A.17: These plots show the area between the 5% and the 50% quantil for all method presented in figure A.15. The plots the kurtosis of the waiting time distribution for the prices being below the respective threshold. To be able to compare it to the kurtosis of an exponential distribution, a line is plotted at $\kappa = 9$.

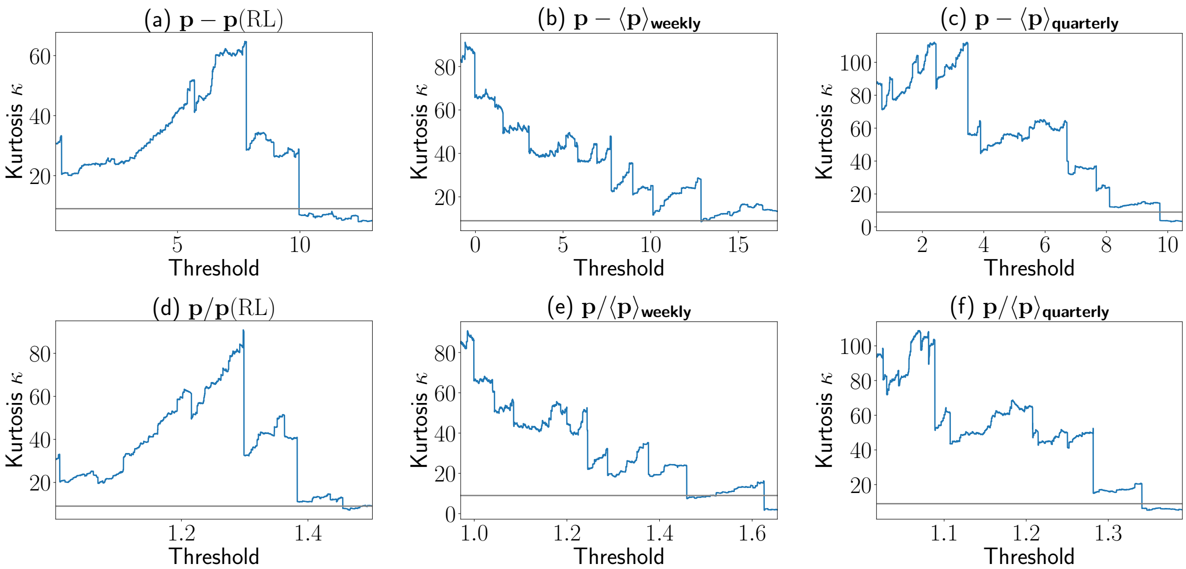

Figure A.18: These plots show the area between the 50% and the 95% quantil for all method presented in figure A.16. The plots the kurtosis of the waiting time distribution for the prices being above the respective threshold. To be able to compare it to the kurtosis of an exponential distribution, a line is plotted at $\kappa = 9$.

Bachelorthesis
Eva Sophia Mix
August 2020